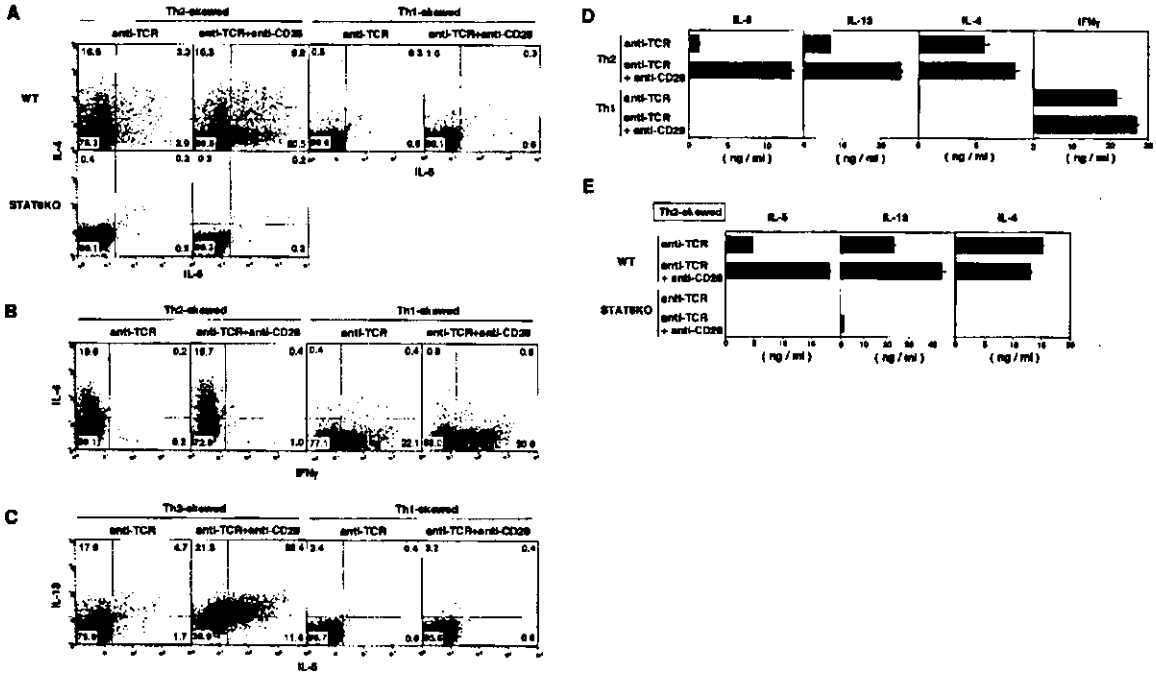

FIG. 1. **Costimulation with anti-CD28 mAb enhanced the generation of IL-5- and IL-13-producing cells.** *A*, *B*, and *C*, freshly prepared splenic CD4 T cells from B6 mice were cultured with immobilized anti-TCR mAb (H57-597, 3 μg/ml) in the presence of costimulation with agonistic anti-CD28 mAb (37.51, 3 μg/ml) under Th1- or Th2-skewed conditions for 7 days. The cultured cells were restimulated, and intracellular IL-5/IL-4, IFNγ/IL-4, and IL-5/IL-13 profiles were determined. The percentages of cells present in the each quadrant are shown. *D* and *E*, CD4 T cells from normal B6 or STAT6-KO mice were cultured under the conditions described above, and restimulation was done with anti-TCR mAb for 8 h. The amounts of IL-5, IL-13, IL-4, and IFNγ in the culture supernatant were measured by ELISA. *WT*, wild type.

CACTGAGCTGCCTGGCGCCGT. A detailed protocol for detection of intergenic transcripts was described previously (34). The primers used are the same as those used in ChIP assay.

RESULTS

Costimulation with Anti-CD28 mAb Enhances the Generation of IL-5- and IL-13-producing Cells—The aim of this study was to clarify the molecular mechanisms that control chromatin remodeling of the IL-5 gene locus during Th2 cell differentiation. We first assessed the role for CD28 costimulation in the generation of IL-5-producing Th2 cells. Freshly prepared CD4 T cells from young adult (4 weeks) B6 mice were cultured *in vitro* with immobilized anti-TCR in the presence of agonistic anti-CD28 mAbs (37.51) to effect stimulation. The IL-5/IL-4 profiles of CD4 T cells cultured under Th1- or Th2-skewed conditions are depicted in Fig. 1*A*. As can be seen, the generation of IL-5-producing cells (both $IL\text{-}5^+IL\text{-}4^-$ and $IL\text{-}5^+IL\text{-}4^+$ fractions) cultured under Th2-skewed conditions was greatly enhanced in the presence of CD28 costimulation. The increased generation of IL-4-producing cells was marginal under these culture conditions. IL-5-producing cells generated with CD28 costimulation were STAT6-dependent and not detected under Th1-skewed culture conditions. The generation of IFNγ-producing Th1 cells was moderately increased by the presence of CD28 costimulation (Fig. 1*B*). The levels of IL-13-producing cells were also increased by the presence of CD28 costimulation (Fig. 1*C*).

Concurrently, the amount of cytokines produced by developing Th2 cells cultured with CD28 costimulation was assessed by ELISA (Fig. 1, *D* and *E*). As expected, CD28 costimulation significantly enhanced the production of IL-5 and IL-13, whereas the effects on the production of IL-4 and IFNγ were marginal. The production of Th2 cytokines (IL-5, IL-13, and IL-4) was all STAT6-dependent regardless of the presence or absence of CD28 costimulation (Fig. 1*E*). Taken together these results suggest that the generation of IL-5- and IL-13-producing cells was Th2-specific, STAT6-dependent, and more sensitive to CD28 costimulation as compared with that of IL-4-producing cells.

Dynamics of Histone H3 Hyperacetylation of the IL-5 Gene Locus in Developing Th2 Cells Cultured with CD28 Costimulation—To clarify whether CD28 costimulation enhances histone hyperacetylation of the IL-5 gene locus during Th2 cell differentiation, we first examined the kinetics of acetylation of the IL-5 promoter, IL-4 promoter, and RAD50 promoter regions using a ChIP assay with anti-acetylhistone H3 Ab. Developing Th1 and Th2 cells cultured with CD28 costimulation were harvested 2, 3.5, 5, and 7 days after stimulation. The results of this analysis are presented as the relative band intensity of each group normalized with band intensity of the corresponding input DNA as shown in the *right panel* of Fig. 2. Two days after stimulation, low but significant levels of increase in acetylation occurred at all of the regions tested, and basically no difference between the three culture conditions was noted. However, as shown in Fig. 2*A*, the levels of histone acetylation associated with the IL-5 promoter increased significantly after cultivation for more than 3 days under Th2 skewed conditions, particularly in those cultures with CD28 costimulation. In contrast, the levels of histone hyperacetylation in the IL-4 promoter were increased day by day, and no significant difference was detected in the presence or absence of CD28 costimulation. The levels of histone hyperacetylation in the RAD50 gene promoter region were increased equivalently under these three culture conditions. These results suggest that histone hyperacetylation of the IL-5 gene locus is more sensitive to CD28

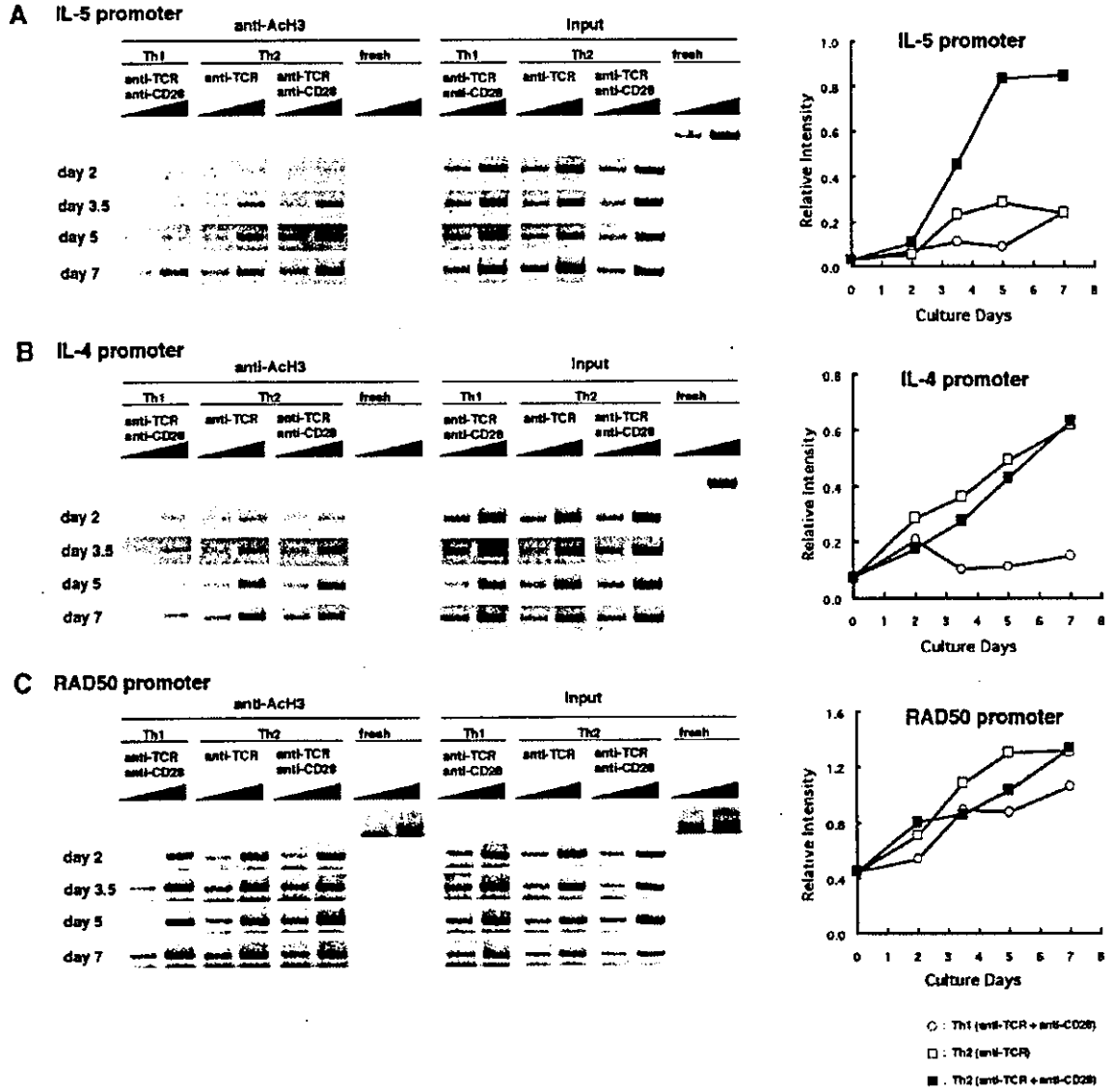

FIG. 2. **Induction of histone H3 hyperacetylation of IL-5, IL-4, and RAD50 gene loci in developing Th2 cells with CD28 costimulation.** Developing Th1 and Th2 cells cultured with immobilized anti-TCR mAb and CD28 costimulation were prepared 2, 3.5, 5, and 7 days after the stimulation. The acetylation status of histone H3 in the nucleosomes associated with the indicated regions was assessed by a ChIP assay with an anti-acetylated histone H3 antibody and specific primer pairs. Before immunoprecipitation for ChIP assay, aliquots of lysates ($\sim 6 \times 10^2$ cell equivalents) were separated for PCR to determine the relative levels of input DNA. 3-Fold serial dilutions were made with both the input DNA and immunoprecipitated DNA samples before PCR. Two independent experiments were performed, and similar results were obtained. Quantitative representations of the results are shown in the *right panels*. The intensities of the bands at the highest concentration were measured by densitometry, and relative intensities (anti-acetyl histone precipitates/input DNA ratio) for each primer pair were calculated.

costimulation than that of the IL-4 locus.

Enhanced Histone Hyperacetylation Induced with CD28 Costimulation Is Observed Only in the IL-5-associated Nucleosomes—Next, we examined the acetylation status of the DNA regions corresponding to IL-5 promoter, IL-5 intron, IL-13 intron, IL-4 promoter, CNS1, IL-4 V_A enhancer, RAD50 promoter, and IFNγ promoter. CNS1 and IL-4 V_A enhancer regions were previously described to contain regulatory elements or DNase I hypersensitive sites (28, 30). Histone hyperacetylation induced in these regions, except for two controls (RAD50 and IFNγ), occurred in a Th2-specific manner as reported previously (34). As can be seen in Fig. 3*A*, the levels of acetylation in the region of IL-5 promoter and IL-5 intron were significantly enhanced by the presence of CD28 costimulation. In contrast, those of other regions were all unaffected. The effect of CD28 costimulation on the histone hyperacetylation within the IL-5 gene loci was analyzed more precisely with a series of primer pairs within the IL-5 genes as shown in Fig. 3*B*. CD28 costimulation significantly enhanced the levels of histone hyperacetylation at all regions within the IL-5 genes tested (Fig. 3*C*).

Next, we assessed the STAT6 dependence of the CD28 costimulation-induced enhancement of the acetylation (Fig. 3*D*). Similar to other regions (IL-13 intron, IL-4 promoter,

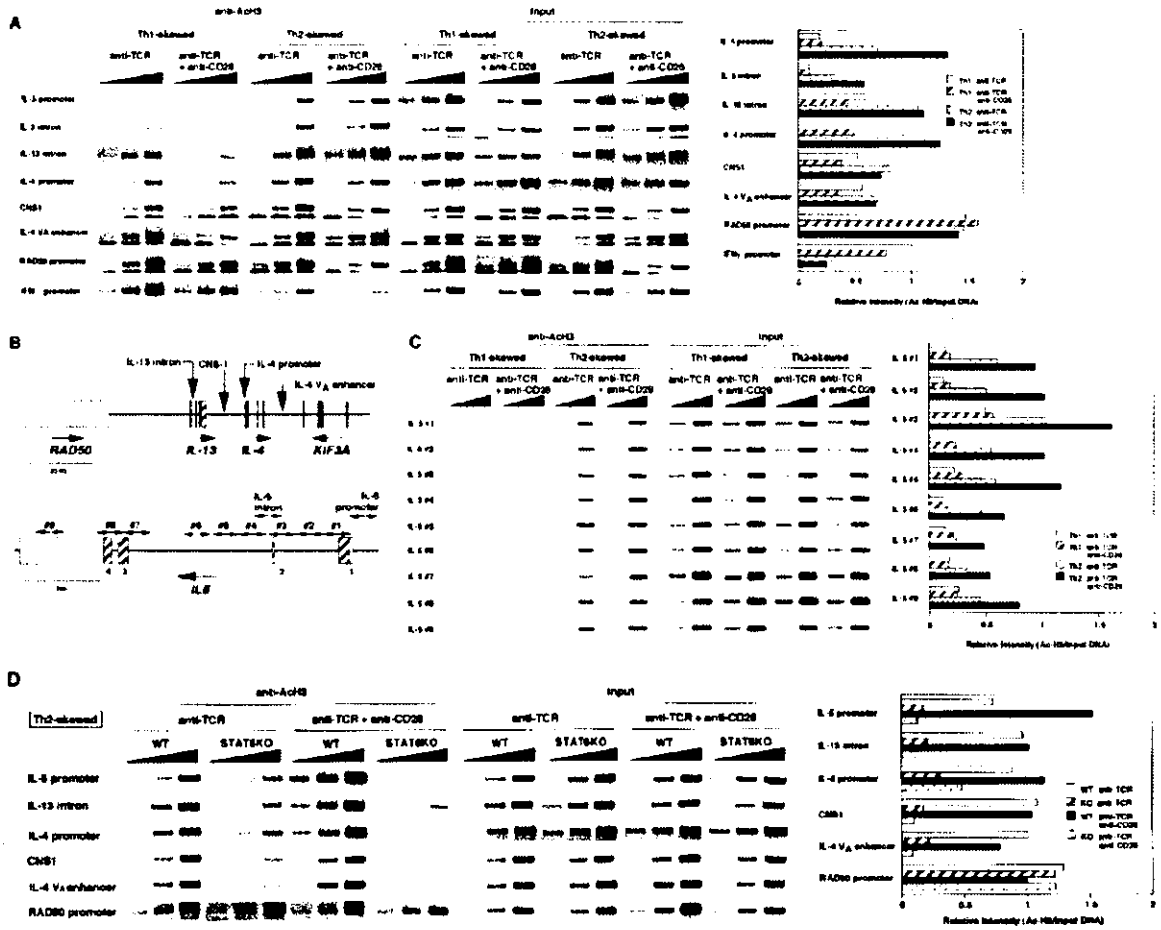

FIG. 3. **Hyperacetylation of histone H3 of the IL-5, IL-13, and IL-4 gene loci in developing Th2 cells cultured with CD28 costimulation.** *A*, developing Th1 and Th2 cells cultured with CD28 costimulation were prepared and subjected to ChIP assays with the indicated primer pairs. 3-Fold serial dilution series were made. The intensity of bands of the highest concentration was measured, and relative intensities are shown in the *right panel*. Similar results were obtained by measuring the bands of intermediate concentration. Three independent experiments with different T cell preparations were performed with similar results. *B*, schematic representation of the IL-5 gene locus and the IL-13 and IL-4 gene loci is shown with the location of the specific primers used in *panel A* and *C*. The location of the primer pairs used in *panel A* is as follows (5′ to 3′). IL-5 promoter F, −521 to −498; IL-5 promoter R, −76 to −101; IL-5 intron F, +857 to +883; IL-5 intron-R, +1214 to +1188. The numbers indicate positions relative to the first nucleotide of the IL-5 exon 1, which is designated as +1. IL-13 intron F, +142/+165; IL-13 intron R, +578 to +555; CNS1 F, +7554 to +7579; CNS1 R, +7767 to +7742. The numbers indicate positions relative to the first nucleotide of the IL-13 exon 1, which is designated as +1. IL-4 promoter F, −661 to −637; IL-4 promoter R, −164 to −187; IL-4 V_A enhancer F, +13234 to +13257; IL-4 V_A enhancer R, +13439 to +13416. The numbers indicate positions relative to the first nucleotide of the IL-4 exon 1, which is designated as +1. RAD50 promoter F, −242 to −217; RAD50 promoter R, −43 to −67. The numbers indicate positions relative to the first nucleotide of the RAD50 exon 1, which is designated as +1. IFNγ promoter F, −3372 to −3349; IFNγ promoter R, −3025 to −3048. The numbers indicate positions relative to the first nucleotide of the IFNγ exon 1, which is designated as +1. *kb*, kilobase. *C*, a ChIP assay with the indicated primer pairs within the IL-5 gene locus was done as in *panel A*. Three independent experiments were performed with similar results. *D*, a ChIP assay with STAT6-KO-developing Th2 cells was done as in *panel A*. Two independent experiments were performed with similar results.

CNS1, and IL-4 V_A enhancer), histone hyperacetylation of the IL-5 promoter locus was not induced in STAT6-KO T cell cultures even in the presence of CD28 costimulation. Thus, STAT6 is critical for the Th2-specific histone hyperacetylation of the IL-5 gene locus induced by anti-TCR stimulation and CD28 costimulation.

Enhanced Production of IL-5 and Histone Hyperacetylation of the IL-5 Gene Locus Induced by CD28 Costimulation Are Dependent on NF-κB Activation—CD28 costimulation is known to induce phosphatidylinositol 3-kinase activation and the subsequent activation of NF-κB. We tested the effect of wortmannin, a phosphatidylinositol 3-kinase inhibitor, on the CD28-induced enhancement of the generation of IL-5-producing cells (43). The generation of IL-5-producing cells in the culture with CD28 costimulation was decreased in the presence of wortmannin in a dose-dependent manner (Fig. 4*A*). In contrast, the generation of IL-4-producing cells was not affected at any doses of wortmannin tested. Concurrently, the effect of wortmannin on the production of cytokines was assessed by ELISA (Fig. 4*B*), and as expected, the enhanced production of IL-5 with CD28 costimulation was sensitive to wortmannin. IL-13 production was also slightly decreased; however, the levels of IL-4 were not changed by the presence of 30 to 300 nM wortmannin.

Next, we assessed the role for NF-κB activation in the CD28-induced enhancement of the generation of IL-5-producing cells and histone hyperacetylation of the IL-5 gene locus. A mutant form of IκBα (IκBαM), which inhibits the NF-κB activation (44), was inserted in an IRES-GFP retroviral construct, and the

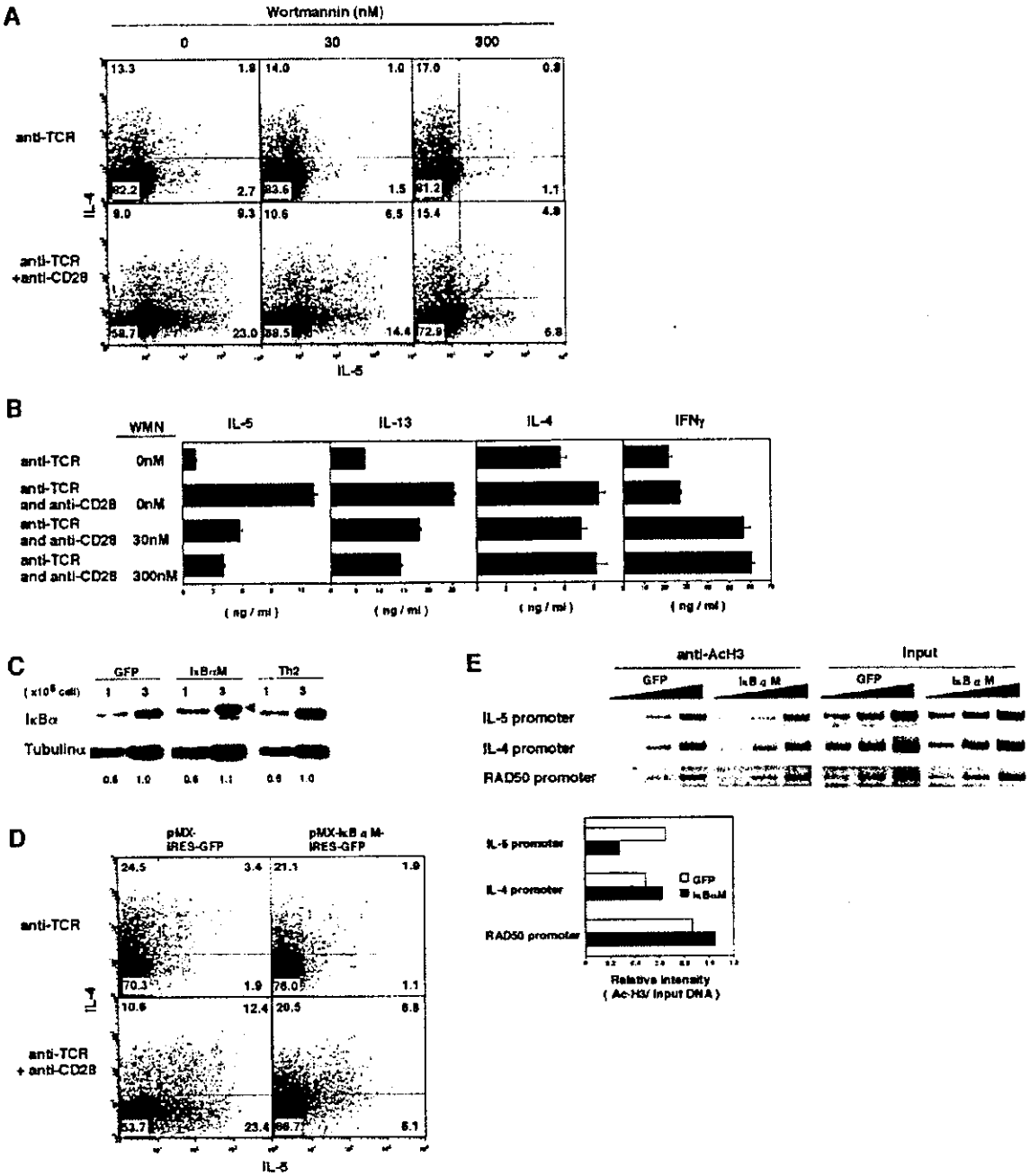

FIG. 4. **Enhanced production of IL-5 and histone hyperacetylation of the IL-5 gene locus induced by CD28 costimulation were dependent on NF-κB activation.** *A*, effect of wortmannin on the generation of IL-5-producing cells under Th2-skewed culture conditions with CD28 costimulation. CD4 T cells were cultured under the conditions described in Fig. 1 in the presence of the indicated doses of wortmannin. The intracellular IL-5/IL-4 profiles are shown. The *numbers* represent the percentages of the cells present in each quadrant. *B*, cytokine production profiles of the cells prepared under the same condition as described in *panel A* are shown. *C*, freshly prepared splenic CD4 T cells were stimulated with anti-TCR and anti-CD28 and infected with a retrovirus pMX-IRES-GFP (*GFP*) or pMX-IκBα-M-IRES-GFP encoding a mutant form of IκBα (*IκBαM*). Seven days after infection GFP$^+$ cells were sorted and subjected to immunoblotting with an anti-IκBα Ab that reacts with both wild type IκBα and IκBαM. The position of IκBαM is indicated by an *arrowhead*. Also non-infected Th2 cells (Th2) were included. Tubulin α was used as a loading control. *D*, freshly prepared splenic CD4 T cells were stimulated under the indicated conditions and infected with a retrovirus encoding a mutant form of IκBα (*IκBαM*) with EGFP. Seven days after infection, the cultured cells were restimulated, and intracellular IL-5/IL-4 profiles of electronically gated GFP positive populations were determined. The percentages of cells present in the each quadrant are shown. *E*, effect of ectopic expression of IκBαM on histone H3 hyperacetylation in IL-5, IL-4, and RAD5 gene loci. Retrovirus-infected CD4 T cells were prepared as described in *panel C*. One million GFP$^+$ infected cells were then collected by cell sorting and the acetylation status of histone H3 was determined by ChIP assay. Relative band intensities measured by densitometry are shown in the *right*. At least three independent experiments were done in each (*A–D*) with similar results.

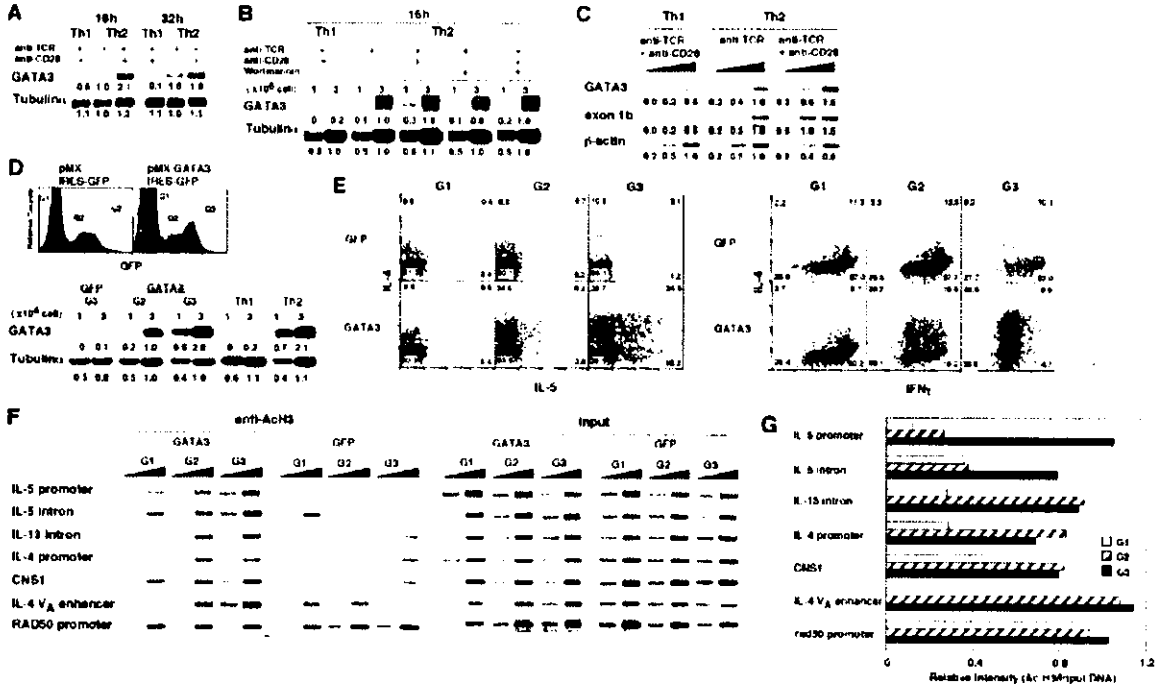

FIG. 5. **The generation of IL-5-producing cells and histone hyperacetylation of the IL-5 gene locus were highly dependent on the expression levels of GATA3.** *A*, freshly prepared CD4 T cells were cultured for 16 and 32 h under the conditions indicated, and the protein expression levels of GATA3 and tubulin α were determined by immunoblotting with specific mAbs. The lysates from 3×10^6 (*upper* for GATA3) and 0.3×10^6 (*lower* for tubulin α) cells were loaded per lane. The results are representative of three independent experiments. Arbitrary densitometric units are depicted under each band. *B*, the effect of wortmannin on the induction of GATA3 was assessed. The experiments as in *panel A* were done in the presence of wortmannin (300 ng/ml). *C*, freshly prepared CD4 T cells were cultured for 12 h under the conditions indicated, and total RNA was prepared. The transcription levels of GATA3, exon 1b of GATA3, and β-actin were determined by semiquantitative RT-PCR analysis with 3-fold serial dilution of template cDNA. Shown are the PCR product bands. Arbitrary densitometric units are indicated. Three independent experiments were done with similar results. *D*, freshly prepared CD4 T cells were stimulated under Th1-skewed conditions and were infected on day 2 with retrovirus encoding GATA3 bicistronically with EGFP (pMx-GATA3-IRES-GFP). The expression levels of GATA3 in the indicated populations sorted using GFP fluorescence were assessed by immunoblotting with anti-GATA3 Ab. Non-infected developing Th1 and Th2 cells were also included for comparison. Arbitrary densitometric units are indicated. *E*, three days after the infection as in *D*, the cells were restimulated, and intracellular IL-5/IL-4 and IFNγ/IL-4 profiles of electronically gated GFP$^-$ (gate G1), GFP^{low} (gate G2), and GFP^{high} (gate G3) populations were determined. The percentages of cells present in the each quadrant are shown. *F*, the cells present in the G1, G2, and G3 gate prepared as in *panel D* were sorted on day 5 by a cell sorter, and the acetylation status of histone H3 was determined by ChIP assay. *G*, relative band intensities (Ac-H3/Input DNA) of each group in *panel E* are shown. The results are representative of three independent experiments.

vectors were introduced into developing Th2 cells cultured with CD28 costimulation. The expression of the introduced IκBαM was confirmed by immunoblotting with an anti-IκBα Ab that reacts with both wild type IκBα and IκBαM (Fig. 4*C*). Substantial amounts of endogenous IκBα were detected in the GFP$^+$ population of mock pMX-IRES-GFP-infected cells (*GFP*) and non-infected Th2 cells (*Th2*). Also, substantial amounts of IκBαM were detected in the IκBαM-infected GFP$^+$ population (*IκBαM*). As previously reported, the *upper band*, indicated by an *arrowhead*, is IκBαM (45). The amount of endogenous IκBα in the IκBαM-infected cells was found to be reduced, probably as a result of the failure of NF-κB activation (46). The percentages of IL-5- and IL-4-producing cells in the GFP-positive infected cell population were determined (Fig. 4*D*). As can be seen, the numbers of IL-5-producing cells were decreased (12.4 ± 23.4 to 6.8 ± 6.1%) by the expression of IκBαM. Interestingly, the percentages of IL-4-producing cells were not significantly affected by IκBαM expression (10.6 ± 12.4 *versus* 20.5 ± 6.8%). The acetylation status of the IL-5 promoter, IL-4 promoter, and RAD50 promoter regions was assessed in the developing Th2 cells infected with IκBαM vector, and significant down-regulation of hyperacetylation in the IL-5-related nucleosomes was detected (Fig. 4*E*). Again, the introduction of IκBαM did not inhibit the acetylation levels of the IL-4- and RAD50-related nucleosomes, suggesting that NF-κB activation is preferentially involved in the process of hyperacetylation of the IL-5 gene locus.

The Generation of IL-5-producing Cells and Histone Hyperacetylation of the IL-5 Gene Locus Are Highly Dependent on the Expression Levels of GATA3—It is reported that the inhibition of NF-κB activity results in reduced GATA3 expression and Th2 cytokine production in developing but not committed Th2 cells (23). To examine the possible involvement of GATA3 in the CD28-induced enhancement of histone hyperacetylation of the IL-5 gene locus, we assessed the protein expression levels of GATA3 in developing Th2 cells cultured with CD28 costimulation. The GATA3 levels were clearly increased by the presence of CD28 costimulation at the 16- and 32-h time points (Fig. 5*A*). The increase was abrogated by the presence of wortmannin (Fig. 5*B*). Furthermore, the transcriptional levels of GATA3 as assessed by semiquantitative RT-PCR were significantly higher in the Th2 cell culture with CD28 costimulation (Fig. 5*C*). We also examined the transcriptional expression of GATA3 exon 1a and 1b (47). Although the expression of exon 1a transcript was undetectable in these developing Th2 cells, that of exon 1b was moderately enhanced in the presence of CD28 costimulation.

To examine the correlation between GATA3 expression and histone hyperacetylation of the IL-5 gene locus, we introduced

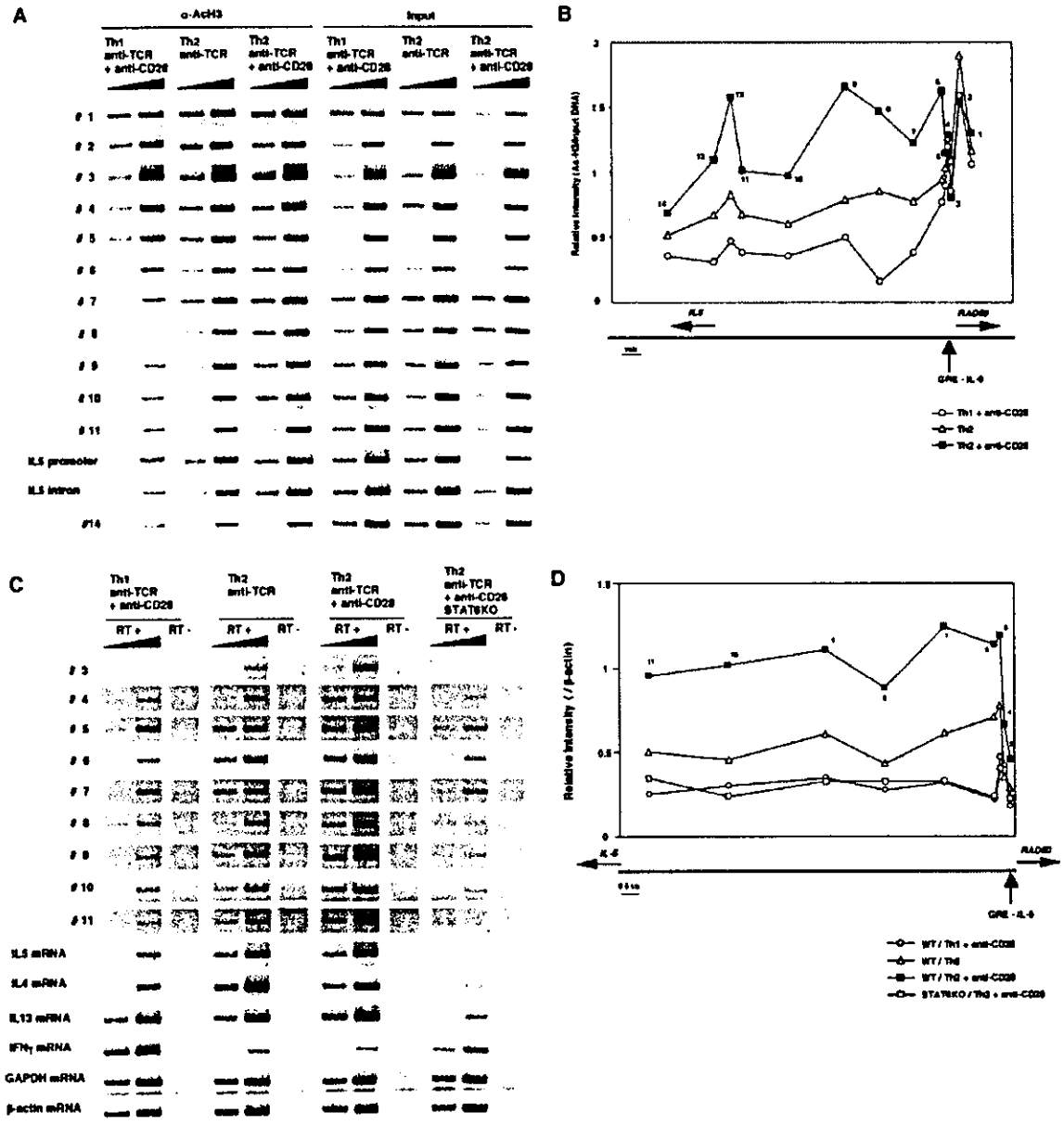

FIG. 6. **Long range histone hyperacetylation and intergenic transcripts in the intergenic region of the IL-5 and RAD50 loci in developing Th2 cells with CD28 costimulation.** *A* and *B*, splenic CD4 T cells were stimulated under the indicated conditions for 7 days, and a ChIP assay was performed. Shown are the PCR product bands for each primer pair (*A*) and the relative band intensities (*B*). The results are representative of three independent experiments. The location of GRE-IL-5 is indicated in *panel B*. *kb*, kilobase. *WT*, wild type. *C* and *D*, freshly prepared CD4 T cells from B6 and STAT6-KO mice were stimulated under the indicated conditions for 2 days and total RNA was prepared. RNA samples were treated with RNase free DNase I to eliminate any possible genomic DNA contamination, reverse-transcribed (RT^+), and then subjected to PCR with the indicated primer pairs. RT^- represents PCR without reverse transcription. *GAPDH*, glyceraldehyde-3-phosphate dehydrogenase. The numbers of the primer pairs are the same as those used in *panel A*. The intensity of bands of the highest concentration was measured, and relative intensities to the β-actin bands are shown in *panel D*. The results are representative of three independent experiments. *E* and *F*, the GATA3 introduced cells as in Fig. 5*D* were sorted (GFP^-, gate G1; GFP^{low}, gate G2; and GFP^{high}, gate G3), and subjected to ChIP assay with indicated primer pairs. The relative intensity (Ac-H3/Input DNA) of each band is shown in *panel F*. The results are representative of two independent experiments.

GATA3 into CD4 T cells stimulated under Th1-skewed conditions using a retroviral vector (pMX-IRES-EGFP) encoding GATA3 bicistronically with EGFP (pMX-GATA3-IRES-EGFP). The expression of GFP and GATA3 protein in the GATA3-infected T cells is depicted in Fig. 5. The expression levels of GATA3 in GFP^{high} (expressing high levels of GATA3, *G3*) population were ~2-fold as compared with those of GFP^{low} (expressing low levels of GATA3, *G2*) population and equivalent to those in Th2 cells. Next, the levels of IL-5- and IL-4-producing cells were compared between GFP^- (no GATA3 expression,

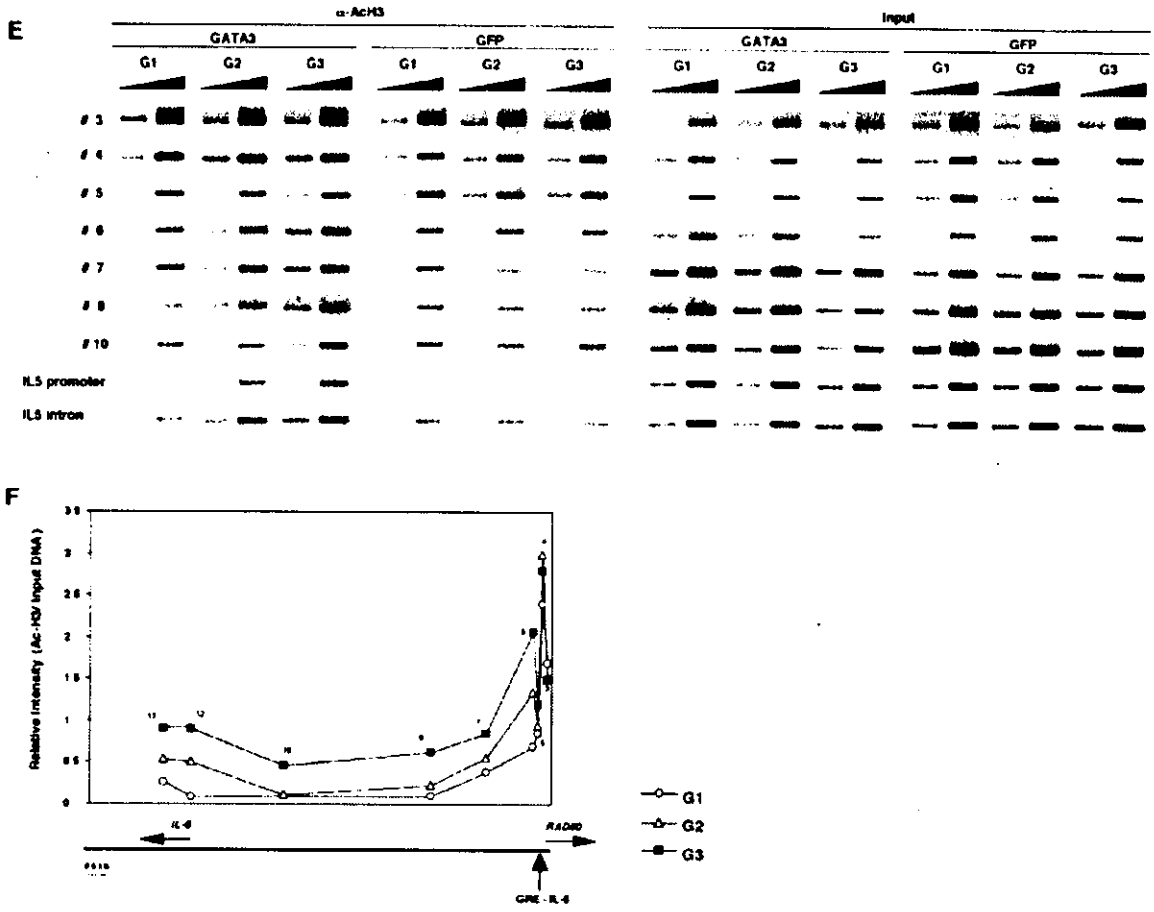

FIG. 6—*continued*

G1), GFP^{low}, and GFP^{high} populations. As shown in Fig. 5*E*, *left panels*, the generation of IL-5-producing cells was greatly increased in the fraction of high GATA3-expressing cells (G3) compared with that of low GATA3-expressing cells (G2) (24.5 ± 18.2 *versus* 8.2 ± 3.8%). The difference in the percentage of IL-5-producing cells was about 4-fold. In contrast, slight (~25%) increases in the generation of IL-4-producing cells were detected (G3, 28.7 ± 24.5%, *versus* G2, 34.6 ± 8.2%). As for the IFNγ-producing cells, a GATA3 dosage-dependent decrease was observed (Fig. 5*E*, *right*). No significant IFNγ/IL-5 double-producing cells were detected (data not shown).

To assess the acetylation status of histones in the GATA3-introduced developing T cells, GFP$^-$, GFP^{low}, and GFP^{high} cells prepared as above were purified by cell sorting and subjected to ChIP assay. Histone hyperacetylation of the Th2 cytokine loci (IL-5 promoter, IL-5 intron, IL-13 intron, IL-4 promoter, CNS1, IL-4 V_A enhancer) was significantly higher in GATA3-expressing cells (G2 and G3) compared with GATA3 non-expressing cells (G1) (Fig. 5*F*). The levels of histone hyperacetylation were increased concomitantly with the increase in the expression of GATA3 (compare G2 and G3) in the IL-5 gene locus (IL-5 promoter and IL-5 intron). No such increase was detected in the IL-4- and IL-13-related nucleosomes. These results suggest that the generation of IL-5-producing cells and histone hyperacetylation of the IL-5 gene locus are highly dependent on the expression levels of GATA3.

Long Range Th2-specific Hyperacetylation Detected in the Intergenic Region of the IL-5 and RAD50 Gene Loci Is Enhanced by the Presence of CD28 Costimulation—A series of primer pairs between the IL-5 and RAD50 loci were generated, and the acetylation status of the nucleosomes associated with IL-5 and RAD50 loci was analyzed. The actual band patterns of each ChIP assay (Fig. 6*A*) and the relative band intensities (Ac-H3/Input DNA) of the 14 selected primer pairs (Fig. 6*B*) are depicted. A long range Th2-specific hyperacetylation was observed from 400 bp upstream of the RAD50 exon 1 (corresponding to primer 5) to the end of IL-5 exon 4 (primer 14). The acetylation levels of all regions tested were significantly increased in the presence of CD28 costimulation. These results indicate that almost all histones from 400 bp upstream of the RAD50 exon 1 to the end of IL-5 exon 4 (primer 14) are selectively hyperacetylated under Th2-skewed culture conditions and are sensitive to CD28 costimulation.

Intergenic Transcription Is Detected throughout the Intergenic Region between the IL-5 and RAD50 Gene Loci—We demonstrated that the intergenic transcription throughout the IL-4 and IL-13 gene loci was accompanied by histone hyperacetylation (34). Thus, we examined the transcription of the intergenic region between the IL-5 and RAD50 gene loci. Interestingly, considerable amounts of transcripts were detected throughout the intergenic region, and the levels were significantly enhanced in the presence of CD28 costimulation (Fig. 6, *C* and *D*). In addition, we examined whether the intergenic transcripts were STAT6-dependent or not. STAT6-deficient CD4 T cells were used in paral-

lel. Only base-line levels of intergenic transcripts were detected. These results suggest that intergenic transcripts are induced throughout the intergenic region between the IL-5 and RAD50 gene loci in a Th2-specific and STAT6-dependent manner and are sensitive to CD28 costimulation.

CD28 Costimulation-sensitive Hyperacetylation in the Intergenic Region of the IL-5 and RAD50 Gene Loci Is Dependent on the Levels of GATA3 Expression—Next, we examined the correlation between the levels of GATA3 expression and histone hyperacetylation of the intergenic region. The retrovirus-induced GATA3-expressing cells shown in Fig. 5*D* were used to compare the acetylation status between GFP^- (no GATA3 expression, G1), GFP^{low} (expressing low levels of GATA3, G2), and GFP^{high} (expressing high levels of GATA3, G3) populations (Fig. 6*E*). The relative intensity (Ac-H3/input DNA) of each acetylation band of GATA3-introduced cells is shown in Fig. 6*F*. As expected, the levels of acetylation in the high GATA3-expressing cells (G3) were significantly higher than those of low and no GATA3-expressing cells (G2 and G1, respectively), suggesting that histone hyperacetylation of the intergenic region requires a high level expression of GATA3.

DISCUSSION

In this report we demonstrated that CD28 costimulation controls Th2-specific histone hyperacetylation of the IL-5 gene locus. CD28-mediated activation of NF-κB and the resulting enhancement of GATA3 induction appeared to be a mechanism by which histone hyperacetylation of the IL-5 gene locus was efficiently induced. This regulation was IL-5 gene-specific because the effect of CD28 costimulation was not observed in the acetylation of the IL-13 or IL-4 gene loci. A long range CD28-sensitive histone hyperacetylation with transcripts was detected in the IL-5 and intergenic region between the IL-5 and RAD50 gene.

The generation of IL-5- and IL-13-producing cells and the production of these cytokines were enhanced by CD28 costimulation of the differentiation culture (Fig. 1). A similar conclusion was drawn from the experiments with wortmannin (Fig. 4, *A* and *B*). As for histone hyperacetylation, however, CD28 costimulation affected only the IL-5 gene locus (Fig. 2 and 3). The transcription of IL-5 and IL-13 is known to be highly dependent on GATA3 as compared with that of IL-4 (11, 48, 49). An efficient transcription of IL-5 or IL-13 may require the enhanced levels of GATA3 that can be achieved by the presence of CD28-costimulation. Thus, it is possible that CD28 costimulation enhanced both histone hyperacetylation and transcription at the IL-5 gene locus but enhanced only transcription at the IL-13 gene. However, it would be unlikely that the enhancement of IL-5 and IL-13 production is mainly due to the effect on transcription, because we did not include anti-CD28 costimulation when the differentiated Th2 cells were restimulated. In fact, the production of IL-4 and IL-5 was only marginally increased when differentiated Th2 cells were restimulated with anti-TCR+anti-CD28.[2] This is consistent with the results reported previously (23).

NF-κB was reported to interact with histone acetyltransferases such as CREB-binding protein/p300 (50–52). In addition, NF-κB binding influenced the recruitment of SWI/SNF-type chromatin remodeling complexes in the granulocyte-macrophage colony-stimulating factor promoter in T cells (53). Thus, it is conceivable that CD28-induced NF-κB activation is involved directly in the acetylation of the IL-5 gene locus at the chromatin level. However, there is no NF-κB binding motif in the intergenic region of the IL-5 and RAD50 gene loci except for one in the promoter region of the IL-5 gene. Thus, it is most likely that the enhanced histone hyperacetylation of the IL-5 gene locus induced by the presence of CD28 costimulation is due to the enhanced expression of GATA3. NF-κB induces a wide variety of genes, such as cytokines (*e.g.* tumor necrosis factor-α and granulocyte-macrophage colony-stimulating factor), chemokines (*e.g.* MCP-1 (monocyte chemoattractant protein)), RANTES (regulated on activation normal T cell expressed and secreted), and eotaxin), and adhesion molecules (*e.g.* ICAM (intercellular adhesion molecule 1) and VCAM (vascular cell adhesion molecule 1) (54, 55). Thus, it is also possible that other genes regulated by NF-κB activation play critical roles in the histone hyperacetylation of the IL-5 gene locus; however, further investigation is required for addressing this issue.

We detected a long range histone hyperacetylation accompanying intergenic transcripts throughout the intergenic region of the IL-5 and RAD50 gene loci (Fig. 6). This is reminiscent of the GATA3-dependent hyperacetylation of the IL-13 and IL-4 gene loci (34, 42), suggesting that a similar molecular mechanism governs the acetylation events of both IL-13/IL-4 and IL-5 genes. The difference was the sensitivity to CD28 costimulation and the dependence on the levels of GATA3. Although the reason for the difference is not clear at this time, the nature of putative GATA response elements responsible for the IL-5 gene acetylation could be distinct from that of conserved GATA3 response element (34). There is 60% homology in the DNA sequence around the upstream region of human RAD50 gene compared with mouse, but we did not identify any conserved GATA binding motifs. However, there are several GATA binding motifs present in both mouse and human, suggesting a possible targeting of GATA3 to this region.

Hyperacetylation of the histone H3 (K9/14) and H4 (K5/8/12/16) is associated with transcriptionally active chromatin (33). However, acetylation of the histone H3-K9/14 does not always correlate with histone H4 acetylation (56). Furthermore, methylation of histone H3-K4 appears to be correlated with active chromatin (57). In the study we focused on the acetylation status of histone H3-K9/14. Thus, further analysis of histone H4 and histone H3-K4 methylation will be required to provide a more detailed view of the chromatin remodeling of the IL-5 gene locus.

In conclusion, we have demonstrated a possible molecular mechanism that controls histone hyperacetylation of the IL-5 gene locus. Characteristic features of chromatin remodeling of the IL-5 gene locus as compared with those of IL-13 and IL-4 were revealed to be the differential involvement of CD28 costimulation and sensitivity to the levels of GATA3 protein. This study is the first to provide evidence that CD28 costimulation controls chromatin remodeling during Th2 cell differentiation.

Acknowledgments—We are grateful to Dr. Ralph T. Kubo for helpful comments and constructive criticisms in the preparation of the manuscript. We also thank Kaoru Sugaya for excellent technical assistance.

[2] M. Inami, M. Yamashita, Y. Tenda, A. Hasegawa, M. Kimura, K. Hashimoto, N. Seki, M. Taniguchi, and T. Nakayama, unpublished observation.

REFERENCES

1. Mosmann, T. R., and Coffman, R. L. (1989) *Annu. Rev. Immunol.* **7**, 145–173
2. Seder, R. A., and Paul, W. E. (1994) *Annu. Rev. Immunol.* **12**, 635–673
3. Reiner, S. L., and Locksley, R. M. (1995) *Annu. Rev. Immunol.* **13**, 151–177
4. Abbas, A. K., Murphy, K. M., and Sher, A. (1996) *Nature* **383**, 787–793
5. Constant, S. L., and Bottomly, K. (1997) *Annu. Rev. Immunol.* **15**, 297–322
6. O'Garra, A. (2000) *Nature* **404**, 719–720
7. Yamashita, M., Hashimoto, K., Kimura, M., Kubo, M., Tada, T., and Nakayama, T. (1998) *Int. Immunol.* **10**, 577–591
8. Yamashita, M., Kimura, M., Kubo, M., Shimizu, C., Tada, T., Perlmutter, R. M., and Nakayama, T. (1999) *Proc. Natl. Acad. Sci. U. S. A.* **96**, 1024–1029
9. Yamashita, M., Katsumata, M., Iwashima, M., Kimura, M., Shimizu, C., Kamata, T., Shin, T., Seki, N., Suzuki, S., Taniguchi, M., and Nakayama, T. (2000) *J. Exp. Med.* **191**, 1869–1879
10. Rengarajan, J., Szabo, S. J., and Glimcher, L. H. (2000) *Immunol. Today* **21**, 479–483

11. Zhang, D. H., Cohn, L., Ray, P., Bottomly, K., and Ray, A. (1997) *J. Biol. Chem.* **272,** 21597–21603
12. Zheng, W., and Flavell, R. A. (1997) *Cell* **89,** 587–596
13. Ouyang, W., Ranganath, S. H., Weindel, K., Bhattacharya, D., Murphy, T. L., Sha, W. C., and Murphy, K. M. (1998) *Immunity* **9,** 745–755
14. Lee, H. J., Takemoto, N., Kurata, H., Kamogawa, Y., Miyatake, S., O'Garra, A., and Arai, N. (2000) *J. Exp. Med.* **192,** 105–115
15. Szabo, S. J., Kim, S. T., Costa, G. L., Zhang, X., Fathman, C. G., and Glimcher, L. H. (2000) *Cell* **100,** 655–669
16. Kubo, M., Yamashita, M., Abe, R., Tada, T., Okumura, K., Ransom, J. T., and Nakayama, T. (1999) *J. Immunol.* **163,** 2432–2442
17. Rulifson, I. C., Sperling, A. I., Fields, P. E., Fitch, F. W., and Bluestone, J. A. (1997) *J. Immunol.* **158,** 658–665
18. June, C. H., Bluestone, J. A., Nadler, L. M., and Thompson, C. B. (1994) *Immunol. Today* **15,** 321–331
19. Ward, S. G., June, C. H., and Olive, D. (1996) *Immunol. Today* **17,** 187–197
20. Kane, L. P., and Weiss, A. (2003) *Immunol. Rev.* **192,** 7–20
21. Lin, X., Cunningham, E. T., Jr., Mu, Y., Geleziunas, R., and Greene, W. C. (1999) *Immunity* **10,** 271–280
22. Rodriguez-Palmero, M., Hara, T., Thumbs, A., and Hunig, T. (1999) *Eur. J. Immunol.* **29,** 3914–3924
23. Das, J., Chen, C. H., Yang, L., Cohn, L., Ray, P., and Ray, A. (2001) *Nat. Immunol.* **2,** 45–50
24. Barnes, P. J., and Karin, M. (1997) *N. Engl. J. Med.* **336,** 1066–1071
25. Yang, L., Cohn, L., Zhang, D. H., Homer, R., Ray, A., and Ray, P. (1998) *J. Exp. Med.* **188,** 1739–1750
26. Donovan, C. E., Mark, D. A., He, H. Z., Liou, H. C., Kobzik, L., Wang, Y., De Sanctis, G. T., Perkins, D. L., and Finn, P. W. (1999) *J. Immunol.* **163,** 6827–6833
27. Agarwal, S., and Rao, A. (1998) *Curr. Opin. Immunol.* **10,** 345–352
28. Loots, G. G., Locksley, R. M., Blankespoor, C. M., Wang, Z. E., Miller, W., Rubin, E. M., and Frazer, K. A. (2000) *Science* **288,** 136–140
29. Mohrs, M., Blankespoor, C. M., Wang, Z. E., Loots, G. G., Afzal, V., Hadeiba, H., Shinkai, K., Rubin, E. M., and Locksley, R. M. (2001) *Nat. Immunol.* **2,** 842–847
30. Agarwal, S., Avni, O., and Rao, A. (2000) *Immunity* **12,** 643–652
31. Bird, J. J., Brown, D. R., Mullen, A. C., Moskowitz, N. H., Mahowald, M. A., Sider, J. R., Gajewski, T. F., Wang, C. R., and Reiner, S. L. (1998) *Immunity* **9,** 229–237
32. Kimura, M., Koseki, Y., Yamashita, M., Watanabe, N., Shimizu, C., Katsumoto, T., Kitamura, T., Taniguchi, M., Koseki, H., and Nakayama, T. (2001) *Immunity* **15,** 275–287
33. Strahl, B. D., and Allis, C. D. (2000) *Nature* **403,** 41–45
34. Yamashita, M., Ukai-Tadenuma, M., Kimura, M., Omori, M., Inami, M., Taniguchi, M., and Nakayama, T. (2002) *J. Biol. Chem.* **277,** 42399–42408
35. Avni, O., Lee, D., Macian, F., Szabo, S. J., Glimcher, L. H., and Rao, A. (2002) *Nat. Immunol.* **3,** 643–651
36. Fields, P. E., Kim, S. T., and Flavell, R. A. (2002) *J. Immunol.* **169,** 647–650
37. Lee, H. J., O'Garra, A., Arai, K., and Arai, N. (1998) *J. Immunol.* **160,** 2343–2352
38. Zhang, D. H., Yang, L., and Ray, A. (1998) *J. Immunol.* **161,** 3817–3821
39. Schwenger, G. T., Fournier, R., Kok, C. C., Mordvinov, V. A., Yeoman, D., and Sanderson, C. J. (2001) *J. Biol. Chem.* **276,** 48502–48509
40. Takeda, K., Tanaka, T., Shi, W., Matsumoto, M., Minami, M., Kashiwamura, S., Nakanishi, K., Yoshida, N., Kishimoto, T., and Akira, S. (1996) *Nature* **380,** 627–630
41. Nakayama, T., June, C. H., Munitz, T. I., Sheard, M., McCarthy, S. A., Sharrow, S. O., Samelson, L. E., and Singer, A. (1990) *Science* **249,** 1558–1561
42. Omori, M., Yamashita, M., Inami, M., Ukai-Tadenuma, M., Kimura, M., Nigo, Y., Hosokawa, H., Hasegawa, A., Taniguchi, M., and Nakayama, T. (2003) *Immunity* **19,** 281–294
43. Ward, S. G., Wilson, A., Turner, L., Westwick, J., and Sansom, D. M. (1995) *Eur. J. Immunol.* **25,** 526–532
44. Traenckner, E. B., Pahl, H. L., Henkel, T., Schmidt, K. N., Wilk, S., and Baeuerle, P. A. (1995) *EMBO J.* **14,** 2876–2883
45. Zhou, M., Gu, L., Zhu, N., Woods, W. G., and Findley, H. W. (2003) *Oncogene* **22,** 8137–8144
46. Sun, S. C., Ganchi, P. A., Ballard, D. W., and Greene, W. C. (1993) *Science* **259,** 1912–1915
47. Asnagli, H., Afkarian, M., and Murphy, K. M. (2002) *J. Immunol.* **168,** 4268–4271
48. Kishikawa, H., Sun, J., Choi, A., Miaw, S. C., and Ho, I. C. (2001) *J. Immunol.* **167,** 4414–4420
49. Lavenu-Bombled, C., Trainor, C. D., Makeh, I., Romeo, P. H., and Max-Audit, I. (2002) *J. Biol. Chem.* **277,** 18313–18321
50. Perkins, N. D., Felzien, L. K., Betts, J. C., Leung, K., Beach, D. H., and Nabel, G. J. (1997) *Science* **275,** 523–527
51. Sheppard, K. A., Rose, D. W., Haque, Z. K., Kurokawa, R., McInerney, E., Westin, S., Thanos, D., Rosenfeld, M. G., Glass, C. K., and Collins, T. (1999) *Mol. Cell. Biol.* **19,** 6367–6378
52. Zhong, H., May, M. J., Jimi, E., and Ghosh, S. (2002) *Mol. Cell* **9,** 625–636
53. Holloway, A. F., Rao, S., Chen, X., and Shannon, M. F. (2003) *J. Exp. Med.* **197,** 413–423
54. Ghosh, S., and Karin, M. (2002) *Cell* **109,** (suppl.) 81–96
55. Li, Q., and Verma, I. M. (2002) *Nat. Rev. Immunol.* **2,** 725–734
56. Johnson, K., Angelin-Duclos, C., Park, S., and Calame, K. L. (2003) *Mol. Cell. Biol.* **23,** 2438–2450
57. Kouzarides, T. (2002) *Curr. Opin. Genet. Dev.* **12,** 198–209

THE JOURNAL OF BIOLOGICAL CHEMISTRY
Vol. 279, No. 26, Issue of June 25, pp. 26983–26990, 2004
Printed in U.S.A.

Essential Role of GATA3 for the Maintenance of Type 2 Helper T (Th2) Cytokine Production and Chromatin Remodeling at the Th2 Cytokine Gene Loci*

Received for publication, April 2, 2004
Published, JBC Papers in Press, April 15, 2004, DOI 10.1074/jbc.M403688200

Masakatsu Yamashita‡§¶, Maki Ukai-Tadenuma‡¶, Takeshi Miyamoto§, Kaoru Sugaya‡§, Hiroyuki Hosokawa§, Akihiro Hasegawa§, Motoko Kimura§, Masaru Taniguchi‖, James DeGregori‡‡, and Toshinori Nakayama§ §§**

*From the ‡PRESTO Project, Japan Science and Technology Corporation (JST), §Department of Immunology, Graduate School of Medicine, Chiba University, 1-8-1 Inohana Chuo-ku, Chiba 260-8670, Japan, the ‖Laboratory for Immune Regulation, RIKEN Research Center for Allergy and Immunology, Yokohama 230-0045, Japan, and the **Department of Biochemistry and Molecular Genetics, University of Colorado Health Sciences Center, BRB802, Denver, Colorado 80262*

GATA3 expression is essential for type-2 helper T (Th2) cell differentiation. GATA3-mediated chromatin remodeling at the Th2 cytokine gene loci, including Th2-specific long range histone hyperacetylation of the interleukin (IL)-13/IL-4 gene loci, occurs in developing Th2 cells. However, little is known about the role of GATA3, if any, in the maintenance of established remodeled chromatin at the Th2 cytokine gene loci. Here, we established a Cre/LoxP-based site-specific recombination system in cultured CD4 T cells using a unique adenovirus-mediated gene transfer technique. This system allowed us to investigate the effect of loss of GATA3 expression in *in vitro* differentiated Th2 cells. After ablation of GATA3, we detected reduced production of all Th2 cytokines, increased DNA methylation at the IL-4 gene locus, and decreased histone hyperacetylation at the IL-5 gene locus but not significantly so at the IL-13/IL-4 gene loci. Thus, GATA3 plays important roles in the maintenance of the Th2 phenotype and continuous chromatin remodeling of the specific Th2 cytokine gene locus through cell division.

After antigenic stimulation, naive CD4 T cells differentiate into two distinct helper T cell (Th)[1] subsets, Th1 and Th2 cells (1). Th1 cells produce IFN-γ to control cell-mediated immunity against intracellular pathogens. Th2 cells produce IL-4, IL-5, and IL-13, and are involved in humoral immunity and allergic reactions (2–4). The outcome of Th cell differentiation depends on the cytokine environment (5, 6). IL-4-mediated STAT6 activation is important for inducing efficient Th2 cell generation (7, 8), although IL-4/STAT6-independent Th2 responses have also been reported in various experimental systems (9–13).

Recent studies have identified several transcription factors that control Th2 cell differentiation (8, 14, 15). Among them, GATA3 appears to be a master transcription factor for Th2 cell differentiation. GATA3 is selectively expressed in Th2 cells and its ectopic expression induces Th2 cell differentiation even in the absence of STAT6 (16–19). Also, GATA3-dependent autoactivation (13, 19) and an instructive role of GATA3 for Th2 cell differentiation (20) were reported.

Changes in the chromatin structure of the Th2 cytokine (IL-4/IL-5/IL-13) gene loci occur during Th2 cell differentiation (14, 21). Th2 cell differentiation induced by ectopic expression of GATA3 results in DNA demethylation (21) and the induction of DNase I-hypersensitive sites in the IL-4 gene locus (19, 22). Recently, we and others demonstrated that histone hyperacetylation of the Th2 cytokine gene loci occurs in developing Th2 cells in a Th2-specific and STAT6-dependent manner (23–25). We demonstrated an essential role for GATA3 in Th2-specific histone hyperacetylation (23). We generated a precise map of the Th2-specific histone hyperacetylation within the type 2 cytokine gene loci, and identified a 71-bp conserved GATA3 response element (CGRE) 1.6 kbp upstream of the IL-13 locus exon 1 (23). The conserved GATA3 response element (CGRE) may play a crucial role for GATA3-mediated targeting and downstream spreading of core histone hyperacetylation within the IL-13 and IL-4 gene loci in developing Th2 cells. However, it is still unclear whether continuous expression of GATA3 is required for the maintenance of the established chromatin remodeling at the Th2 cytokine gene loci.

In the present study, we investigated the role for GATA3 in the maintenance of Th2 cytokine production and the remodeled chromatin using a newly established *in vitro* site-specific recombination system. The loss of GATA3 expression resulted in decreased Th2 cytokine production, reduction of histone hyperacetylation at the IL-5 gene locus, and increased DNA methylation at the IL-4 gene locus. Thus, GATA3 plays important roles in the maintenance of the Th2 phenotype and continuous chromatin remodeling of the specific Th2 cytokine gene loci.

* This work was supported by Ministry of Education, Culture, Sports, Science and Technology (Japan) Grants-in-Aid for Scientific Research, Priority Areas Research 13218016, 12051203, Scientific Research B 14370107, and Special Coordination Funds for Promoting Science and Technology, the Ministry of Health, Labor and Welfare (Japan), the Program for Promotion of Fundamental Studies in Health Science of the Organization for Pharmaceutical Safety and Research (Japan), Uehara Memorial Foundation, Hamaguchi Foundation, and Kanae Foundation. The costs of publication of this article were defrayed in part by the payment of page charges. This article must therefore be hereby marked "*advertisement*" in accordance with 18 U.S.C. Section 1734 solely to indicate this fact.

¶ Both authors contributed equally to this study.

‡‡ Supported by a Scholar award from the Leukemia and Lymphoma Society and National Institutes of Health NCI Grant RO1 CA77314.

§§ To whom correspondence should be addressed: Dept. of Immunology, Graduate School of Medicine, Chiba University, 1-8-1 Inohana, Chuo-ku, Chiba 260-8670 Japan. Tel.: 81-43-226-2200; Fax: 81-43-227-1498; E-mail: tnakayama@faculty.chiba-u.jp.

[1] The abbreviations used are: Th, helper T; TCR, T cell antigen receptor; STAT, signal transducer and activator of transcription; CAR, coxsackie/adenovirus receptor; EGFP, enhanced green fluorescence protein; ChIP, chromatin immunoprecipitation; STAT6-KO, signal transducer and activator of transcription 6-deficient; IL, interleukin; mAb, monoclonal antibody; GFP, green fluorescent protein; ELISA, enzyme-linked immunosorbent assay; Ad, adenovirus; IFU, infection units; PE, phycoerythrin.

EXPERIMENTAL PROCEDURES

Mice—C57BL/6 mice were purchased from SLC (Shizuoka, Japan). STAT6-deficient mice were kindly provided by Dr. Shizuo Akira (Osaka University, Japan) (26). Transgenic mice expressing coxsackie/adenovirus receptor under the control of an *lck* proximal promoter (coxsackie/adenovirus receptor (CAR) Tg mice) has been previously described (27). All mice used in this study were maintained under specific pathogen-free conditions and were used at 4–6 weeks of age. Animal care was in accordance with the guidelines of Chiba University.

Immunofluorescent Staining and Flow Cytometry Analysis—In general, one million cells were stained with antibodies as indicated according to a standard method (28). Anti-CD4-fluorescein isothiocyanate (RM4-1-FITC) and anti-CD8-PE (53.6-72-PE) were purchased from BD Pharmingen. For detecting hCAR, biotinylated anti-CAR antibody (RmcB) (27) and Cy5-conjugated avidin were used. For intracellular staining, allophycocyanin-conjugated anti-IFN-γ antibody (XMG1.2; BD Pharmingen), anti-IL-5 antibody (TRFK5; BD Pharmingen), and PE-conjugated anti-IL-4 antibody (11B11; BD Pharmingen) were used (29, 30). Flow cytometry analysis was performed on FACScalibur (BD Biosciences) and results were analyzed with CELLQUEST software (BD Biosciences).

In Vitro T Cell Differentiation Culture—Purification and *in vitro* Th cell differentiation cultures were done as described (23, 29). Splenic CD4 cells were purified using magnetic beads and an Auto-MACS Sorter™ (Miltenyi Biotec), yielding purity of >98%. For Th1 differentiation, the cells (1.5×10^6) were stimulated for 2 days with immobilized anti-TCR mAb (H57-597; BD Pharmingen) and anti-CD28 mAb (37.51; BD Pharmingen) in the presence of IL-2 (25 units/ml), IL-12 (100 units/ml), and anti-IL-4 mAb (11B11, 25% culture supernatant). For Th2 cell differentiation, cells were stimulated with immobilized anti-TCR mAb and anti-CD28 mAb for 2 days in the presence of IL-2 (25 units/ml), IL-4 (100 units/ml), and anti-IFNγ mAb (R4-6A2, 25% culture supernatant). The cells were then transferred to new wells and cultured for another 3 days in the presence of only the cytokines present in the initial culture. In some experiments, two or three cycles of the anti-TCR plus anti-CD28 stimulation were used.

Virus Vectors, Infection, and Strategy for Deletion of GATA3 Transgene—The retroviral vector pMX-IRES-EGFP and a Plat-E packaging cell line were kindly provided by Dr. Toshio Kitamura (University of Tokyo, Tokyo, Japan). Retrovirus vectors containing a *loxP*-flanked EGFP cassette (pMX-loxP-EGFP-loxP) and a *loxP*-flanked human GATA3-IRES-EGFP cassette (pMX-loxP-GATA3-IRES-EGFP-loxP) were generated using the original pMX-IRES-GFP vector (31) (Fig. 1*A*). The method for the preparation of virus supernatant was described previously (32). An adenovirus vector containing a Cre recombinase expression cassette (Ad-Cre) was kindly provided by Izumi Saito (University of Tokyo, Tokyo, Japan) (Fig. 1*B*) (33).

To investigate the effect of loss of GATA3 expression in differentiated Th2 cells, we established a site-specific recombination system in CD4 T cells cultured *in vitro*. The strategy of introduction and deletion of the GATA3 transgene is illustrated in Fig. 1*C*. First, naive CD4 T cells were stimulated under Th1-skewed conditions, and infected with retrovirus vectors containing a *loxP*-flanked GATA3/IRES/EGFP cassette. Three days later, GFP-positive retrovirus-infected cells were sorted with a FACSVantage (BD Biosciences) flow cytometer and restimulated under the same Th1-skewed conditions of initial stimulation for a further 5 days. After another cycle of 5-day re-stimulation culture under Th1-skewed conditions, the cells were infected with Ad-Cre to delete the GATA3/IRES/EGFP transgene by expressing NLS-tagged Cre recombinase. The preparation of adenovirus supernatant was done as described (33). Cell entry by adenovirus involves high-affinity binding of the viral fiber capsid protein to a cellular receptor, CAR. We used CAR Tg mouse T cells to avoid the limited expression of CAR on T cells (27).

In Figs. 4 and 5, a more strict protocol was used. The outline of the protocol is shown in Fig. 4*A*. Four days after infection of retrovirus vectors containing a *loxP*-flanked GATA3/IRES/EGFP, cells were stimulated with immobilized anti-TCR and anti-CD28 for 4 h, stained with anti-IL-4 PE detection mAbs using IL-4 Secretion Assay kit (number 130-090-515: Militenyi Biotec), and $GFP^+IL\text{-}4^+$ cells were sorted with purity >98%. The sorted cells were cultured for 6 days in the presence of cytokines (IL-2 and IL-12), and then another stimulation with anti-TCR and anti-CD28 was performed. Two days later, cells were infected with Ad-Cre. Four days after Ad-Cre infection, GFP^- cells were sorted to exclude the small numbers of GFP^+ (GATA3) expressing cells remaining in the culture. After T cell expansion by anti-TCR stimulation, analysis was done on day 25. To exclude the effect of endogenously induced GATA3 molecules, we used naive STAT6-deficient CD4 T cells and Th1-skewed culture conditions containing anti-IL-4 mAb throughout the 25-day cultivation.

PCR Analysis—The levels of EGFP transgene were assessed by semi-quantitative PCR with a specific primer pairs: forward, GTGAACCGTCAGATCCG-3′ and reverse, 5′-TTACTTGTACAGCTCGTC.

Immunoblot Analysis—The amounts of GATA3 and GFP were assessed by immunoblotting with anti-GATA3 mouse mAb, HG3-31 (Santa Cruz Biotechnology, Santa Cruz, CA), and anti-GFP antiserum (MBL, Nagoya, Japan) as described (30).

ELISA for the Measurement of Cytokine Concentration—Cells were stimulated with immobilized anti-TCR (3 μg/ml) in 48-well flat bottom plates (2.5×10^6 cells/well) for 24 h at 37 °C. The production of IL-4, IL-5, IFN-γ, and IL-2 was assessed by ELISA as described previously (30). The production of IL-13 was evaluated with a mouse IL-13 ELISA kit (R & D Systems) according to the manufacturer's protocol.

Reverse Transcriptase-PCR—Total RNA was isolated from cultured cells using the TRIzol reagent. Reverse transcription was carried out with Superscript II RT (Invitrogen). Three-fold serial dilutions of template cDNA were done. The primers used were as described previously (32).

Chromatin Immunoprecipitation (ChIP) Assay—ChIP assays were performed using histone H3 ChIP assay kits (number 17-245; Upstate Biotechnology) and specific primers as described previously (23).

Methylation-specific PCR—Genomic DNA was isolated from 1×10^6 cells by using a Wizard Genomic DNA Purification kit (Promega). Bisulfate treatment of DNA was performed by using a CpGenome DNA Modification kit (Intergen, Purchase, NY). The sequences of primers used for PCR amplification were described previously by Guo *et al.* (34).

RESULTS

Efficient Adenovirus-mediated Transgene Introduction into CAR Tg CD4 T Cells in Vitro—The aim of this study was to determine the role of GATA3, if any, in the maintenance of the established Th2 phenotype and Th2-type chromatin remodeling. To investigate the effect of loss of GATA3 expression in differentiated Th2 cells, we established a Cre/loxP-mediated site-specific recombination system in T cells. The system constitutes (i) retrovirus-mediated introduction of a *loxP*-flanked GATA3 transgene for Th2 cell differentiation from naive CD4 T cells, and (ii) subsequent adenovirus-mediated Cre expression to delete the *loxP*-flanked GATA3 transgene (Fig. 1).

Thus, we first evaluated the feasibility of adenovirus-mediated gene transfer in T cells. Naive CD4 T cells express limited amounts of CAR and are known to be resistant to adenovirus infection. To increase the efficiency of adenovirus infection in T cells, we used CAR Tg mice expressing CAR on T cells under the control of the proximal promoter of *lck* and a CD2 enhancer, in which the majority of CD4 and CD8 T cells in the spleen showed high level cell surface expression of CAR (27). Freshly prepared CD4 T cells from CAR Tg mice were infected with Ad-EGFP. Two days after infection, the majority of CAR Tg CD4 T cells expressed substantial levels of GFP compared with that of non-Tg B6 CD4 T cells (Fig. 2*A*). A time course of the GFP expression after Ad-EGFP infection was assessed in CAR CD4 T cells cultured under Th1- or Th2-skewed conditions (Fig. 2*B*). The expression of GFP peaked on day 3 in either Th1 or Th2-skewed culture conditions. The high-level expression was maintained for at least 4 days after infection. Thus, adenovirus-mediated gene transfer was efficient when using CD4 T cells from CAR Tg mice.

Deletion of a loxP-flanked EGFP Transgene by Ad-Cre Infection in Cultured CD4 T Cells—The efficiency of Cre-mediated DNA recombination was next assessed in CAR Tg CD4 T cells using EGFP as an indicator. CAR Tg CD4 T cells were stimulated with anti-TCR mAb plus anti-CD28 mAb and infected with a retrovirus containing a *loxP*-flanked EGFP cassette (pMX-loxP-EGFP-loxP). GFP-expressing infected cells were sorted, restimulated for 3 days, and then infected with either 1 or 3×10^8 IFU of Ad-Cre as described under "Experimental Procedures." Fig. 3*A* shows a representative genomic DNA PCR result assessing the amount of EGFP transgene DNA left in

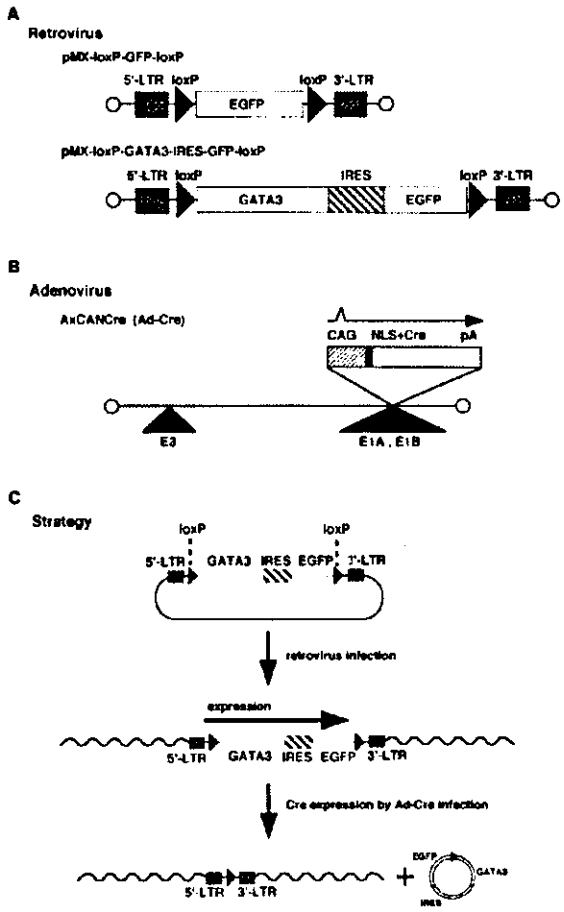

FIG. 1. **Schematic representation of retrovirus and adenovirus vectors, and strategy for Cre-mediated site-specific gene recombination.** *A*, retrovirus vectors containing *loxP*-flanked EGFP (pMX-loxP-EGFP-loxP) and *loxP*-flanked human GATA3-IRES-EGFP (pMX-loxP-GATA3-IRES-EGFP-loxP). *B*, an adenovirus vector inserted with the Cre recombinase gene (*Ad-Cre*). *C*, the strategy for introduction and deletion of the GATA3 transgene.

CD4 T cells after Ad-Cre infection. The ratio of EGFP/input DNA is shown in Fig. 3*B*. The EGFP transgene content was significantly decreased 2 days after Ad-Cre infection in a virus-dosage dependent manner. On day 3, the majority of the EGFP transgene was deleted by infection with 3×10^8 IFU of Ad-Cre (Fig. 3*A*, *bottom*). These results suggest that the *lox-P*-flanked EGFP transgene was efficiently deleted in cultured CD4 T cells by Ad-Cre infection when CAR Tg CD4 T cells are used.

Concurrently, the expression levels of EGFP protein after Ad-Cre infection were monitored by flow cytometry. To allow comparison with the EGFP-negative T cell control peak, no GFP sorting was done in this particular experiment. Shown are representative flow cytometry histograms (Fig. 3*C*), and relative intensity data from the GFP-positive peaks after infection with 3×10^8 IFU of Ad-Cre (Fig. 3*D*). As can be seen, expression levels of GFP in CAR Tg CD4 T cells decreased day by day after Ad-Cre infection, and were approximately one-fifth of the original expression level on day 4 when 3×10^8 IFU of Ad-Cre were used (Fig. 3*D*). In contrast, only a marginal decrease was observed in non-Tg CD4 T cell cultures. Although almost complete deletion of the EGFP transgene was detected on day 3 post-infection with 3×10^8 IFU of Ad-Cre (see Fig. 3, *A* and *B*), a significant amount of GFP protein (~20–30%) was detected by flow cytometry. This could be explained by the substantially long half-life of the GFP protein.

Efficient Depletion of Retrovirus-induced GATA3 Expression by Ad-Cre Infection in in Vitro Differentiated Th2 Cells—To investigate the role of GATA3 in the maintenance of the Th2 phenotype, CD4 T cells from STAT6-deficient CAR Tg mice cultured under Th1-skewed conditions were infected with retroviral vectors containing a *lox-P*-flanked GATA3/IRES/GFP cassette (pMx-loxP-GATA3-IRES-GFP-loxP). In the STAT6-deficient T cells cultured under Th1-skewed conditions, endogenous GATA3 induction was minimum. The outline of the protocol is shown in Fig. 4*A*. Four days after infection of the retrovirus vector, the cells were stimulated with immobilized anti-TCR and anti-CD28 mAb, stained with anti-IL-4-PE detection mAbs, and $GFP^+IL\text{-}4^+$ cells were sorted. Representative GFP/IL-4 profiles are shown in Fig. 4*B*. The sorted cells were cultured for 6 days in the presence of cytokines (IL-2 and IL-12), and another cycle of stimulation with anti-TCR and anti-CD28 was performed on day 12. Two days later, the cells were infected with Ad-Cre (3×10^8 IFU). Four days after Ad-Cre infection, GFP^- cells were sorted to enrich for GATA3 transgene-depleted cells. Th1-skewed conditions were used throughout the 25-day culture. The cultured cells were harvested, and the expression levels of EGFP and GATA3 were assessed to confirm that GATA3 protein is depleted (Fig. 4, *C* and *D*). As can be seen, the levels of GFP fluorescence were reduced (Fig. 4*C*), and the expression levels of GATA3 protein were decreased dramatically (about 10-fold) in the cells infected with Ad-Cre (Fig. 4*D*). Without Ad-Cre infection, the expression of GATA3 protein was not changed during the last 7-day cultivation (data not shown).

The mRNA levels of several transcriptional regulators (GATA3, c-Maf, JunB, and T-bet) in the Th2 cells after ablation of GATA3 were assessed (Fig. 4*E*). As expected, the mRNA levels of GATA3 were ~1/10 of those of LacZ-infected control cells. In contrast, essentially no significant change in c-Maf or JunB expression was detected in the Ad-Cre-infected T cells. The expression of T-bet was reduced by the expression of GATA3, and restored by the depletion of GATA3 transgene.

Expression of GATA3 Is Required for Th2 Cytokine Production in in Vitro Differentiated Th2 Cells—Cytokine production profiles of the cells prepared in Fig. 4 were assessed by cytoplasmic staining. As can be seen in Fig. 5*A*, *middle panels*, more than 40% (39.3 + 3.5%) of the cells infected with pMx-loxP-GATA3-IRES-GFP-loxP were IL-4 producing cells, and more than 30% (19.2 + 18.2%) were IL-5 producing cells. Marginal numbers of IFN-γ producing IL-4 non-producing cells were detected (7.0%). The percentages of IL-4 producing cells were decreased to about 25% (23.1 + 3.8%) after Ad-Cre infection, and those of IL-5 were about 16% (8.1 + 7.9%) (compare the percentages depicted in the *middle* and *right panels* in IFN-γ/IL-4 and IL-5/IL-4 profiles). A significant number of IFN-γ producing cells was noted, suggesting that some of the cells become IFN-γ producing cells after depletion of the GATA3 transgene. These results suggest that GATA3 expression is important for the maintenance of Th2 cytokine production.

Next, the levels of Th2 cytokines produced in the culture supernatant were determined by ELISA. Little in the way of Th2 cytokines (IL-4, IL-13, and IL-5) were detected in supernatants from non-infected cells cultured under Th1-skewed conditions. In contrast, GATA3-transduced cells produced large amounts of Th2 cytokines and decreased amounts of Th1 cytokines (IFN-γ and IL-2) as previously reported (16–19). As

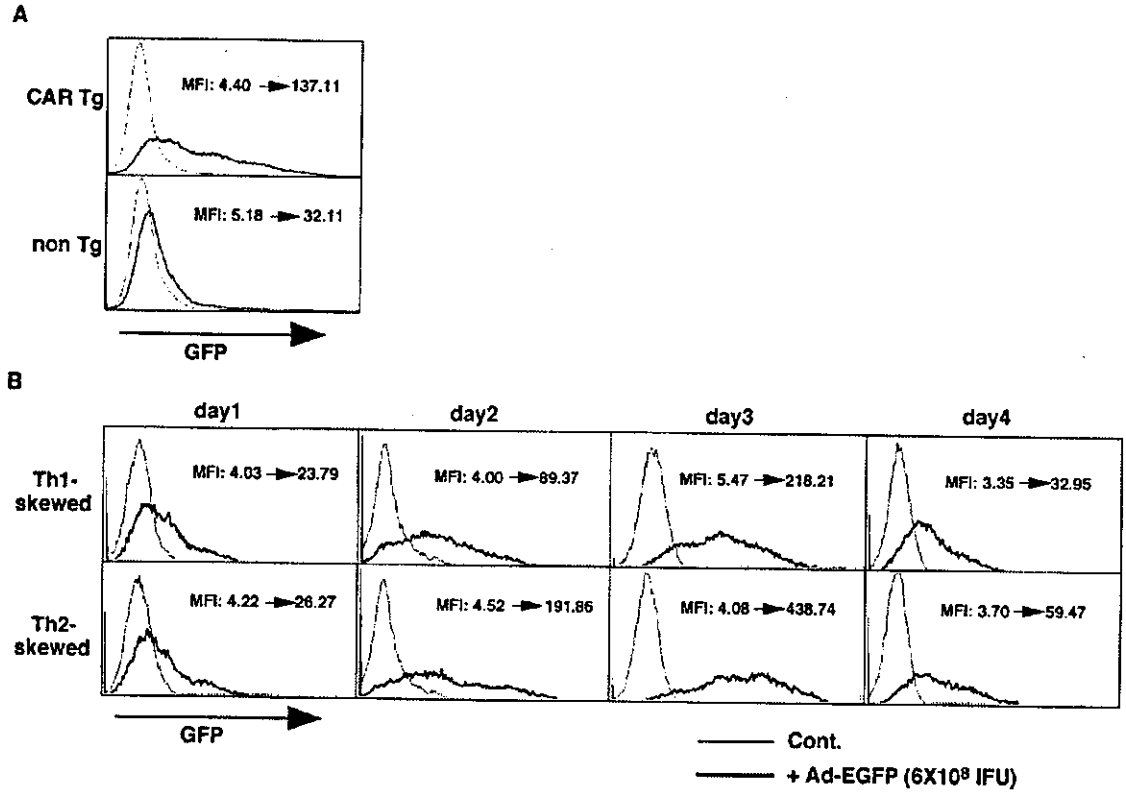

FIG. 2. **Efficient transgene introduction into CAR Tg CD4 T cells using adenovirus vector.** The EGFP gene was cloned into the adenovirus vector (*Ad-EGFP*). Freshly prepared CAR Tg and normal non-Tg CD4 T cells (*A*) and cultured CAR CD4 T cells under Th1- and Th2-skewed conditions were infected with Ad-EGFP. Assays were done on day 2 (*A*) or on the indicated day (*B*) after Ad-EGFP infection. The efficiency of Ad-EGFP transgene expression was assessed in flow cytometry using GFP fluorescence as an indicator. Mean fluorescence intensity (*MFI*) is depicted in each panel.

expected, the production of Th2 cytokines (IL-4, IL-13, and IL-5) was significantly decreased by Ad-Cre infection (Fig. 5*B*, *bottom*). IFN-γ production was moderately restored. These results suggest that the continuous expression of GATA3 is important for the production of IL-4, IL-5, and IL-13 in the *in vitro* differentiated Th2 cells.

GATA3 Is Required for the Maintenance of Hyperacetylation of Histone H3 in the IL-5 Gene Locus but Not in the IL-13/IL-4 Gene Loci—Finally, we assessed the chromatin remodeling status of the Th2 cytokine gene loci after deletion of the GATA3 transgene. Acetylation status of histone H3 (K9/14) in the nucleosomes associated with the Th2 cytokine gene loci was determined by ChIP assays. The levels of acetylation in *in vitro* differentiated Th2 cells cultured under Th2-skewed conditions for 5 days are shown for comparison. The relative band intensities (Ac-H3/Input DNA) are shown in Fig. 6*B*. As we reported previously, ectopic expression of GATA3 induced histone hyperacetylation in the Th2 cytokine gene loci (Fig. 6*A*, *Ac-H3*, *second column*) (23). As shown in Fig. 6, *A* and *B*, significantly reduced histone hyperacetylation of the IL-5 promoter region was detected by the Ad-Cre-mediated deletion of the GATA3 transgene. The decrease in the acetylation of IL-4 promoter, IL-13 promoter, V_A enhancer, CNS1, and GATA3 response element was marginal. Acetylation of the IFNγ promoter was decreased by GATA3 expression, and significantly increased by deletion of the GATA3 transgene (Fig. 6, *A* and *B*, *bottom*).

GATA3 Is Required for the Maintenance of Continuous Demethylation of the IL-4 Intron 2 Region—Demethylation of the IL-4 intron 2 region in developing Th2 and established Th2 cells was reported previously (21). Here, we used a methylation-specific PCR technique to evaluate the methylation status of IL-4 intron 2 (34). After treatment of genomic DNA with bisulfate, unmethylated cytidine is converted to uridine but methylcytidine is preserved as cytidine. In this system, primers that distinguish uridine (thymidine) and cytidine at sites of CpGs were used to evaluate the levels of methylation. We focused on two cytidine residues within the IL-4 intron 2 region, and four patterns (both methylated, M/M; one methylated and one demethylated, M/U or U/M; and both demethylated, U/U) would be detected. In GATA3 non-transduced cells, 50% of the genome contained methylated cytidine at both residues (Fig. 6, *C* and *D*, *top*). In GATA3-transduced cells, only 20% of this region was methylated at both residues, 40% was unmethylated and 40% was hemimethylated (Fig. 6, *C* and *D*, *middle*). When the GATA3 transgene was deleted, 50% of the genome contained both cytidine residues methylated, and only 20% was unmethylated (Fig. 6, *C* and *D*, *bottom*), suggesting that the methylation pattern was compatible to that of non-GATA3 transduced cells. These results suggest that continuous GATA3 expression is required to maintain the unmethylated status of the Th2 cytokine gene loci in differentiated Th2 cells.

DISCUSSION

In the present study, we established a Cre/LoxP-based site-specific recombination system in cultured CD4 T cells using a unique adenovirus-mediated gene transfer technique. Ectopic

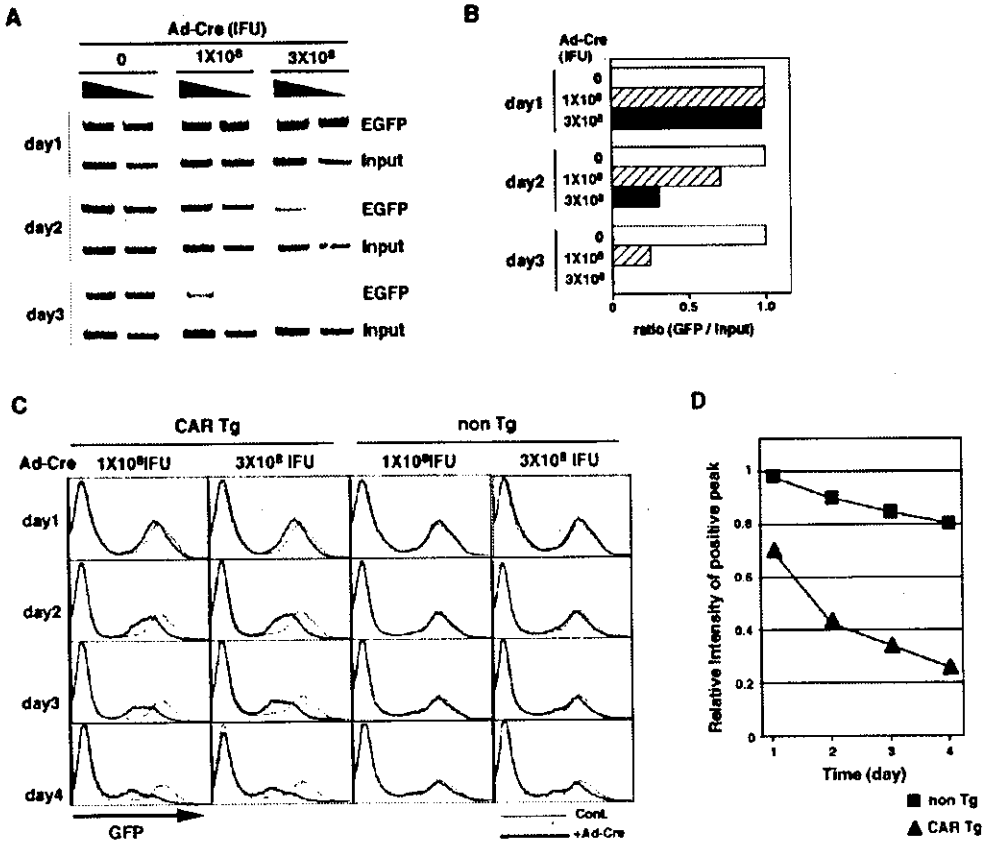

FIG. 3. **Deletion of a *loxP*-flanked EGFP transgene by Ad-Cre infection in cultured CD4 T cells.** CAR Tg CD4 T cells were stimulated with anti-TCR mAb plus anti-CD28 mAb and infected with a retrovirus containing *loxP*-flanked EGFP (pMX-loxP-EGFP-loxP). GFP expressing infected cells were sorted, restimulated for 3 days, and then infected with 1×10^8 or 3×10^8 IFU of Ad-Cre. *A*, a representative genomic semi-quantitative PCR of the EGFP transgene. *B*, the ratios of EGFP/input DNA. *C*, CAR Tg and non-Tg CD4 T cells were stimulated with anti-TCR mAb plus anti-CD28 mAb, and infected with a retrovirus containing *loxP*-flanked EGFP (pMX-loxP-EGFP-loxP). The expression levels of GFP protein in whole cells (both retrovirus-infected and uninfected populations) were monitored by flow cytometry after 1×10^8 and 3×10^8 IFU Ad-Cre infection. The relative intensity of the positive peak of 3×10^8 IFU Ad-Cre infection is depicted in *panel D*.

expression of GATA3 induced Th2 cell generation without IL-4 or STAT6 activation. Using these Th2 cells, the role of GATA3 expression in the maintenance of Th2 phenotype was examined by deleting the GATA3 transgene with adenovirus-mediated expression of the Cre protein. The reduction of GATA3 expression in the *in vitro* differentiated Th2 cells resulted in decreased production of all Th2 cytokines tested (IL-4, IL-13, and IL-5) (Fig. 5), decreased histone hyperacetylation of the IL-5 gene locus (Fig. 6, *A* and *B*), and increased methylation of DNA at the IL-4 intron 2 region (Fig. 6, *C* and *D*). These results suggest that continuous expression of GATA3 is required for the maintenance of Th2 cytokine production and remodeled open chromatin at the specific Th2 cytokine gene loci.

The production of Th2 cytokines, particularly IL-5 and IL-13, were reported to be highly dependent on the transcriptional activity of GATA3 (16, 35, 36). We reported that expression of GATA3 induced more than a 10-fold increase in IL-5 and IL-13 promoter activities, whereas that of the IL-4 promoter was increased only about 2-fold (23). Therefore, the decreased IL-5 and IL-13 production after deletion of the GATA3 transgene by Cre-induced recombination is explained at least in part by the decreased transcriptional activity of GATA3.

More importantly, however, we detected decreased histone hyperacetylation at the IL-5 gene locus and increased methylation of IL-4 gene intron 2 following GATA3 ablation (Fig. 6), suggesting that the levels of openness of chromatin at specific Th2 cytokine gene loci were dependent on the expression of GATA3. Interestingly, the levels of acetylation at the IL-13/IL-4 gene loci were not significantly affected by the ablation of the GATA3 protein (Fig. 6). It is possible that small amounts of residual GATA3 are sufficient for the maintenance of acetylation of the IL-13/IL-4 gene loci but not for that of the IL-5 locus. Alternatively, GATA3 independent molecular events that maintain the histone hyperacetylation are operating at the IL-13/IL-4 gene loci in differentiated Th2 cells. Histone H3-K4 methylation and histone H3-K9/14 acetylation appear to be associated with transcriptionally active chromatin (37). Disruption of an H3-K4-specific methyltransferase, MLL containing a SET domain, resulted in reduced histone acetylation (38, 39). Thus, unknown but critical molecular events may control histone H3-K9/14 acetylation as well as histone H3-K4 methylation in *in vitro* differentiated Th2 cells.

Recently, we have reported that the induction of histone hyperacetylation at the IL-5 gene locus is dependent on STAT6 and GATA3, but the signal requirements are distinct from that for the IL-13/IL-4 gene loci (40). The remodeling process of the IL-5 gene locus is more sensitive to CD28-induced NF-κB activation. It is possible that molecular events governing the maintenance of histone hyperacetylation of the IL-13/IL-4 gene loci and that of IL-5 locus are distinct.

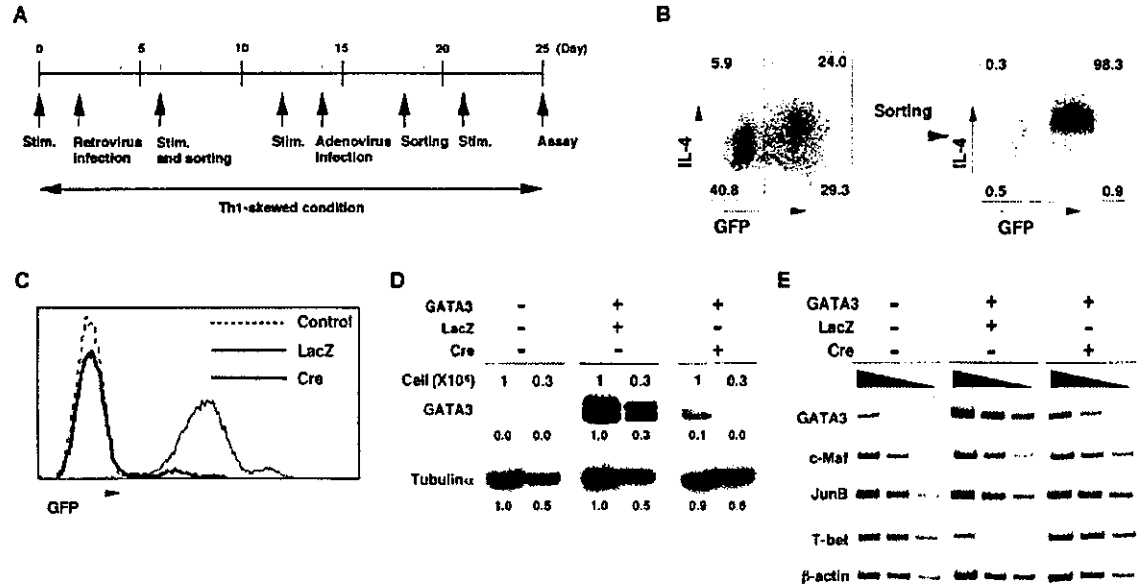

FIG. 4. **Depletion of retrovirus-induced GATA3 expression by Ad-Cre infection in *in vitro* differentiated Th2 cells.** *A*, the outline of the protocol for GATA3-depletion in Th2 cells. Naive CD4 T cells from CAR Tg mice with a STAT6-deficient background were stimulated (*stim.*) under Th1-skewed conditions, and infected with retrovirus vectors containing a *loxP*-flanked GATA3/IRES/EGFP cassette on day 2. Four days after infection with retrovirus vectors, the cells were stimulated with immobilized anti-TCR and anti-CD28 for 4 h, stained with anti-IL-4 PE detection mAbs, and GFP$^+$IL-4$^+$ cells were sorted. The sorted cells were cultured for 6 days in the presence of cytokines (IL-2 and IL-12), and another stimulation with anti-TCR and anti-CD28 was performed. Two days later, the cells were infected with either Ad-Cre (3×10^8 IFU) or Ad-LacZ (3×10^8 IFU). Four days after adenovirus infection, GFP$^-$ cells were sorted to enrich the GATA3 transgene-depleted cells. After T cell expansion by anti-TCR/anti-CD28 stimulation, analysis was done on day 25. *B*, representative GFP/IL-4 profiles on sorted cells at day 6. Cells were stained with anti-IL-4 PE as described in *A* and GFP/IL-4 double positive cells were sorted by flow cytometry. The percentages of cells in each quadrant are shown. *C*, expression levels of EGFP in the *in vitro* differentiated Th2 cells with or without Ad-Cre infection. An Ad-LacZ vector was used as a control. The expression level of EGFP in the cells (on day 25) prepared as in *panel A* was determined by flow cytometry. *D*, immunoblot analysis for GATA3 in the *in vitro* differentiated Th2 cells with or without Ad-Cre infection. GATA3 and tubulin α expression levels were determined by immunoblotting with specific mAbs. Lysates from 3×10^6 (*upper* for GATA3) and 0.3×10^6 (*lower* for tubulin α) cells were used per lane. The results are representative of three independent experiments. Arbitrary densitometric units are depicted under each band. *E*, expression levels of Th2- and Th1-related transcriptional regulators in Th2 cells depleted of the GATA3 transgene. The transcription levels of GATA3, c-Maf, JunB, T-bet, and β-actin were determined by semiquantitative reverse transcriptase-PCR analysis with 3-fold serial dilution of template cDNA.

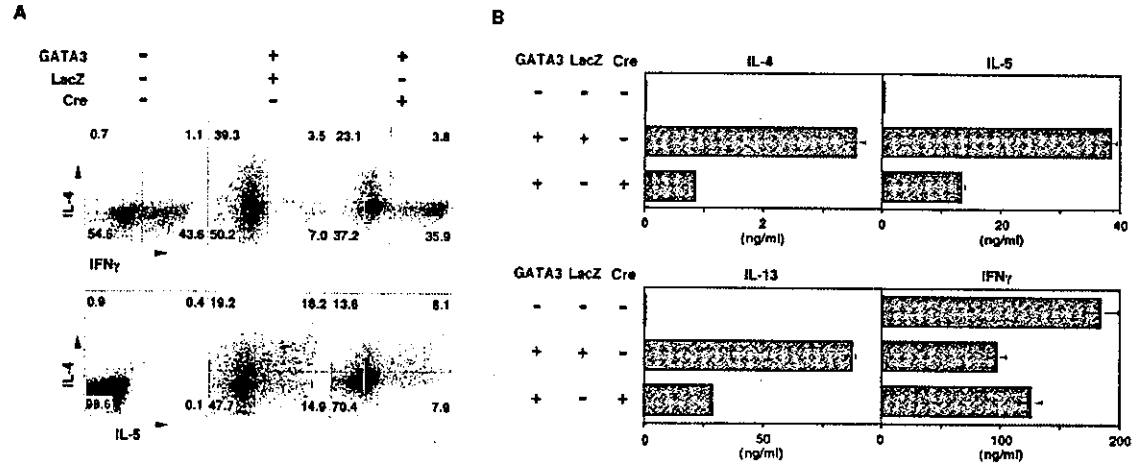

FIG. 5. **Effect of GATA3 depletion on Th2 cytokine production in *in vitro* differentiated Th2 cells.** *A*, cytokine production profiles of Th2 cells after depletion of the GATA3 transgene prepared as in Fig. 4*A* were assessed by cytoplasmic staining (IFN-γ/IL-4 and IL-5/IL-4). The percentages of the cells present in each quadrant are shown. Four independent experiments were done with similar results. *B*, cytokine production of Th2 cells after depletion of the GATA3 transgene was assessed by ELISA. Four independent experiments were done with similar results.

We also demonstrated that GATA3 expression is required for the maintenance of demethylation of the IL-4 intron 2 region (Fig. 6, *C* and *D*). It is not clear whether GATA3 is involved directly in the methylation processes of the methyltransferase complex at this time. Recently, Tamaru *et al.* (42) reported that methylation of lysine 9 of histone H3 is a mark for DNA

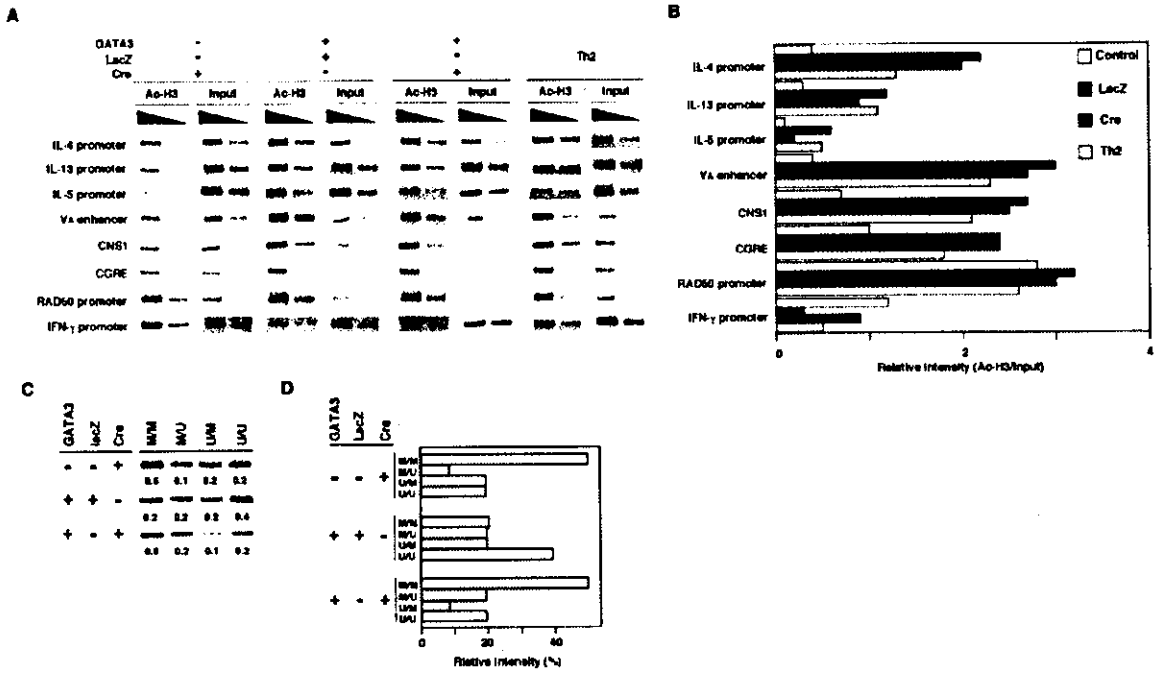

FIG. 6. **The role for GATA3 in the maintenance of open chromatin at the Th2 cytokine gene loci.** *A*, the acetylation status of histone H3 in nucleosomes associated with the Th2 cytokine gene loci was determined by ChIP assay. An Ad-LacZ vector was used as a control for Ad-Cre. Histone hyperacetylation of IL-4-, IL-13-, and IL-5-associated nucleosomes (IL-4 promoter, IL-13 promoter, IL-5 promoter, V_A enhancer, CNS1 and GATA3 response element) in Th2 cells after depletion of the GATA3 transgene prepared as in Fig. 4*A* was examined. The levels of acetylation in 5-day *in vitro* differentiated Th2 cells are also shown for comparison. Three independent experiments were done with similar results. *B*, the relative intensity of histone hyperacetylation (Ac-H3/Input DNA for the higher concentration bands) in each group shown in *panel A*. *C*, the DNA methylation status of the IL-4 intron 2 region assessed by a methylation-specific PCR technique. We focused on two cytidine residues within the IL-4 intron 2 region, and four patterns (both methylated, *M/M*; one methylated and one demethylated, *M/U* or *U/M*; and both demethylated, *U/U*) were detected. Three independent experiments were done with similar results. *D*, relative intensity (%) of each band shown in *panel C*.

methylation in *Neurospora crassa* (41). Also very recently, a tight correlation between methylation of lysine 9 of histone H3 and DNA methylation was reported in mammalian cells (42). Finally, it has been reported in many systems that there is an inverse correlation between acetylation and methylation of histone H3 lysine 9 in chromatin activation (43–45). Thus, it is likely that GATA3 is required solely for selective targeting of the histone acetyltransferase complex to the Th2 cytokine gene loci, and that this causes the appearance of demethylation indirectly. Whereas Hutchins *et al.* (46) reported that GATA3 is not required for the induction of DNA demethylation of intron 2 of the IL-4 gene locus, we detected demethylation of one site in the same intron 2 region by ectopic expression of GATA3 (Fig. 6). The reason for this apparent discrepancy is not clear, but it is possible that the PCR detection system we used here, to assess demethylation at specific sites in the IL-4 intron 2 region, may be more sensitive than the Southern blotting method used by Hutchins *et al.* (46).

In Fig. 4, the levels of residual GATA3 after Cre introduction appeared to be about 10% of control. However, the numbers of IL-4 or IL-5 producing cells and the levels of actual cytokine production were only reduced 2–3-fold (Fig. 5, *A* and *B*). These results may suggest that a certain low level of GATA3 protein is enough to maintain Th2 cytokine gene expression in some cells. It is also possible that the Th2 phenotype is already fixed in certain numbers of Th2 cells, in which unknown GATA3-independent mechanisms control the maintenance of the Th2 phenotype.

Murphy and colleagues (13) reported that the expression of GATA3 is controlled by autoactivation. Two distinct promoters control the expression of GATA3 (47). A newly identified promoter is suggested to be responsible for GATA3-dependent GATA3 transcription (GATA3 autoactivation). Thus, we performed Northern blot analysis to assess endogenous GATA3 levels, and could not detect any endogenous GATA3 after deletion of the *loxP*-flanked GATA3 transgene.[2] One possible explanation is that the expression level of GATA3 after *in vitro* site-specific recombination was too low to activate a GATA3-dependent promoter. In any event, the effect of deletion of the GATA3 transgene could not have been complicated in any way by the expression of endogenous GATA3 protein that might have been induced by so called autoactivation, as there was no endogenous GATA3 expression.

In our Cre/LoxP-based site-specific recombination system, the retrovirus-introduced transgene was deleted from the genome quite efficiently by adenovirus-mediated Cre introduction (Fig. 3, *A* and *B*). Thus, this system has proven to be a powerful tool for studying stage-specific roles of GATA3, and may be useful in this regard with various factors that are crucial for T cell activation, differentiation, and function. In summary, we demonstrated an important role for GATA3 in the maintenance of Th2 cytokine production, and remodeled

[2] M. Yamashita, M. Ukai-Tadenuma, T. Miyamoto, K. Sugaya, H. Hosokawa, A. Hasegawa, M. Kimura, M. Taniguchi, J. DeGregori, and T. Nakayama, unpublished observation.

open chromatin at the specific Th2 cytokine gene loci using a newly established *in vitro* site-specific recombination system.

Acknowledgment—We are grateful to Dr. Pandelakis A. Koni (Medical college of Georgia) for helpful comments and constructive criticisms in the preparation of the manuscript.

REFERENCES

1. Mosmann, T. R., and Coffman, R. L. (1989) *Annu. Rev. Immunol.* **7,** 145–173
2. Abbas, A. K., Murphy, K. M., and Sher, A. (1996) *Nature* **383,** 787–793
3. Constant, S. L., and Bottomly, K. (1997) *Annu. Rev. Immunol.* **15,** 297–322
4. O'Garra, A. (2000) *Nature* **404,** 719–720
5. Seder, R. A., and Paul, W. E. (1994) *Annu. Rev. Immunol.* **12,** 635–673
6. Reiner, S. L., and Locksley, R. M. (1995) *Annu. Rev. Immunol.* **13,** 151–177
7. Nelms, K., Keegan, A. D., Zamorano, J., Ryan, J. J., and Paul, W. E. (1999) *Annu. Rev. Immunol.* **17,** 701–738
8. Murphy, K. M., Ouyang, W., Farrar, J. D., Yang, J., Ranganath, S., Asnagli, H., Afkarian, M., and Murphy, T. L. (2000) *Annu. Rev. Immunol.* **18,** 451–494
9. Dent, A. L., Hu-Li, J., Paul, W. E., and Staudt, L. M. (1998) *Proc. Natl. Acad. Sci. U. S. A.* **95,** 13823–13828
10. Kaplan, M. H., Wurster, A. L., Smiley, S. T., and Grusby, M. J. (1999) *J. Immunol.* **163,** 6536–6540
11. Finkelman, F. D., Morris, S. C., Orekhova, T., Mori, M., Donaldson, D., Reiner, S. L., Reilly, N. L., Schopf, L., and Urban, J. F., Jr. (2000) *J. Immunol.* **164,** 2303–2310
12. Jankovic, D., Kullberg, M. C., Noben-Trauth, N., Caspar, P., Paul, W. E., and Sher, A. (2000) *J. Immunol.* **164,** 3047–3055
13. Ouyang, W., Lohning, M., Gao, Z., Assenmacher, M., Ranganath, S., Radbruch, A., and Murphy, K. M. (2000) *Immunity* **12,** 27–37
14. Agarwal, S., and Rao, A. (1998) *Curr. Opin. Immunol.* **10,** 345–352
15. Rengarajan, J., Szabo, S. J., and Glimcher, L. H. (2000) *Immunol. Today* **21,** 479–483
16. Zhang, D. H., Cohn, L., Ray, P., Bottomly, K., and Ray, A. (1997) *J. Biol. Chem.* **272,** 21597–21603
17. Zheng, W., and Flavell, R. A. (1997) *Cell* **89,** 587–596
18. Ouyang, W., Ranganath, S. H., Weindel, K., Bhattacharya, D., Murphy, T. L., Sha, W. C., and Murphy, K. M. (1998) *Immunity* **9,** 745–755
19. Lee, H. J., Takemoto, N., Kurata, H., Kamogawa, Y., Miyatake, S., O'Garra, A., and Arai, N. (2000) *J. Exp. Med.* **192,** 105–115
20. Farrar, J. D., Ouyang, W., Lohning, M., Assenmacher, M., Radbruch, A., Kanagawa, O., and Murphy, K. M. (2001) *J. Exp. Med.* **193,** 643–650
21. Bird, J. J., Brown, D. R., Mullen, A. C., Moskowitz, N. H., Mahowald, M. A., Sider, J. R., Gajewski, T. F., Wang, C. R., and Reiner, S. L. (1998) *Immunity* **9,** 229–237
22. Takemoto, N., Kamogawa, Y., Jun Lee, H., Kurata, H., Arai, K. I., O'Garra, A., Arai, N., and Miyatake, S. (2000) *J. Immunol.* **165,** 6687–6691
23. Yamashita, M., Ukai-Tadenuma, M., Kimura, M., Omori, M., Inami, M., Taniguchi, M., and Nakayama, T. (2002) *J. Biol. Chem.* **277,** 42399–42408
24. Avni, O., Lee, D., Macian, F., Szabo, S. J., Glimcher, L. H., and Rao, A. (2002) *Nat. Immunol.* **3,** 643–651
25. Fields, P. E., Kim, S. T., and Flavell, R. A. (2002) *J. Immunol.* **169,** 647–650
26. Takeda, K., Tanaka, T., Shi, W., Matsumoto, M., Minami, M., Kashiwamura, S., Nakanishi, K., Yoshida, N., Kishimoto, T., and Akira, S. (1996) *Nature* **380,** 627–630
27. Wan, Y. Y., Leon, R. P., Marks, R., Cham, C. M., Schaack, J., Gajewski, T. F., and DeGregori, J. (2000) *Proc. Natl. Acad. Sci. U. S. A.* **97,** 13784–13789
28. Nakayama, T., June, C. H., Munitz, T. I., Sheard, M., McCarthy, S. A., Sharrow, S. O., Samelson, L. E., and Singer, A. (1990) *Science* **249,** 1558–1561
29. Yamashita, M., Kimura, M., Kubo, M., Shimizu, C., Tada, T., Perlmutter, R. M., and Nakayama, T. (1999) *Proc. Natl. Acad. Sci. U. S. A.* **96,** 1024–1029
30. Omori, M., Yamashita, M., Inami, M., Ukai-Tadenuma, M., Kimura, M., Nigo, Y., Hosokawa, H., Hasegawa, A., Taniguchi, M., and Nakayama, T. (2003) *Immunity* **19,** 281–294
31. Nosaka, T., Kawashima, T., Misawa, K., Ikuta, K., Mui, A. L., and Kitamura, T. (1999) *EMBO J.* **18,** 4754–4765
32. Kimura, M., Koseki, Y., Yamashita, M., Watanabe, N., Shimizu, C., Katsumoto, T., Kitamura, T., Taniguchi, M., Koseki, H., and Nakayama, T. (2001) *Immunity* **15,** 275–287
33. Kanegae, Y., Takamori, K., Sato, Y., Lee, G., Nakai, M., and Saito, I. (1996) *Gene (Amst.)* **181,** 207–212
34. Guo, L., Hu-Li, J., Zhu, J., Watson, C. J., Difilippantonio, M. J., Pannetier, C., and Paul, W. E. (2002) *Proc. Natl. Acad. Sci. U. S. A.* **99,** 10623–10628
35. Kishikawa, H., Sun, J., Choi, A., Miaw, S. C., and Ho, I. C. (2001) *J. Immunol.* **167,** 4414–4420
36. Lavenu-Bombled, C., Trainor, C. D., Makeh, I., Romeo, P. H., and Max-Audit, I. (2002) *J. Biol. Chem.* **277,** 18313–18321
37. Kouzarides, T. (2002) *Curr. Opin. Genet. Dev.* **12,** 198–209
38. Nishioka, K., Chuikov, S., Sarma, K., Erdjument-Bromage, H., Allis, C. D., Tempst, P., and Reinberg, D. (2002) *Genes Dev.* **16,** 479–489
39. Zegerman, P., Canas, B., Pappin, D., and Kouzarides, T. (2002) *J. Biol. Chem.* **277,** 11621–11624
40. Inami, M., Yamashita, M., Tenda, Y., Hasegawa, A., Kimura, M., Hashimoto, K., Seki, N., Taniguchi, M., and Nakayama, T. (March 23, 2004) *J. Biol. Chem.* 10.1074/jbc.M401248200
41. Tamaru, H., Zhang, X., McMillen, D., Singh, P. B., Nakayama, J., Grewal, S. I., Allis, C. D., Cheng, X., and Selker, E. U. (2003) *Nat. Genet.* **34,** 75–79
42. Lehnertz, B., Ueda, Y., Derijck, A. A., Braunschweig, U., Perez-Burgos, L., Kubicek, S., Chen, T., Li, E., Jenuwein, T., and Peters, A. H. (2003) *Curr. Biol.* **13,** 1192–1200
43. Grewal, S. I., and Moazed, D. (2003) *Science* **301,** 798–802
44. Goll, M. G., and Bestor, T. H. (2002) *Genes Dev.* **16,** 1739–1742
45. Lachner, M., and Jenuwein, T. (2002) *Curr. Opin. Cell Biol.* **14,** 286–298
46. Hutchins, A. S., Mullen, A. C., Lee, H. W., Sykes, K. J., High, F. A., Hendrich, B. D., Bird, A. P., and Reiner, S. L. (2002) *Mol. Cell* **10,** 81–91
47. Asnagli, H., Afkarian, M., and Murphy, K. M. (2002) *J. Immunol.* **168,** 4268–4271

Brief report

Role of a NK receptor, KLRE-1, in bone marrow allograft rejection: analysis with KLRE-1–deficient mice

Eiko Shimizu, Junzo Koike, Hiroshi Wakao, Ken-ichiro Seino, Haruhiko Koseki, Terutaka Kakiuchi, Toshinori Nakayama, and Masaru Taniguchi

Natural killer (NK) cells play a pivotal role in the immune reaction during the bone marrow allograft rejection. Little is known, however, about the molecular mechanisms underlying the NK cell–mediated allograft recognition and rejection. In this report, we assessed the role of a recently identified NK receptor, killer cell lectinlike receptor 1 (KLRE-1), by generating knockout mice. KLRE-1–deficient mice were born at an expected frequency and showed no aberrant phenotype on growth and lymphoid development. Nevertheless, KLRE-1–deficient cells showed a severely compromised allogeneic cytotoxic activity compared with the wild-type cells. Furthermore, allogeneic bone marrow transfer culminated in colony formation in the spleen of KLRE-1–deficient mice, whereas no colony formation was observed in wild-type recipient mice. These results demonstrate that KLRE-1 is a receptor mediating recognition and rejection of allogeneic target cells in the host immune system. (Blood. 2004;104: 781-783)

Introduction

Natural killer (NK) cells play a pivotal role in the recognition and rejection of allogeneic target cells, such as bone marrow (BM) allografts.[1-3] NK cell cytotoxicity is exquisitely controlled by signals emanating from stimulatory and inhibitory NK receptors, which recognize major histocompatibility complex (MHC) class I–related molecules on the target cells.[3,4] The function of NK receptor(s) in allograft rejection has been mainly probed with the aid of monoclonal antibodies (mAbs). It is shown that blocking the inhibitory receptor, CD94/NKG2A with anti-CD94 mAb enhances the cytotoxicity of C57BL/6 NK cells against BALB/c concanavalin A (Con A) blasts,[5] while anti–Ly-49D mAb treatment results in suppression of the BM graft rejection.[6] In both cases, however, it is still open to question whether the effect of anti-CD94 or anti-Ly49D mAbs was direct or attributed to the cross-reactivity of mAbs with other family members.[5,7-10]

Recently, a novel NK receptor, KLRE-1 (also known as NKG2I), belonging to the killer cell lectinlike receptors (KLRs) family has been characterized.[11-13] A series of experiments using anti–KLRE-1 mAbs indicate that this receptor plays a role in the cytotoxicity mediated by NK cells in vitro.[12,13] However, the definitive assessment for the functions of KLRE-1 has to await KLRE-1–deficient mice.

To this end, we have generated KLRE-1 knock-out mice and assessed the role of KLRE-1. KLRE-1–deficient cells showed little cytolytic activity against allogeneic lymphocytes. Furthermore, allogeneic bone marrow transfer resulted in significant colony formation in the spleen of KLRE-1–deficient mice. These results further confirm that KLRE-1 is a crucial NK receptor for recognition and rejection of bone marrow allograft.

Study design

Mice

C57BL/6, BALB/c mice were from Charles River Japan (Yokohama, Japan), and 129/svJ mice were from Jackson Laboratory (Bar Harbor, ME). KLRE-1 knock-out mice have been backcrossed 6 times to C57BL/6 mice. Mice were kept under the specific pathogen-free conditions, and 6- to 8-week-old mice were used for the experiments. All experiments were performed in accordance with the guidelines of Chiba University.

Construction and establishment of EGFP–KLRE-1 knock-in mice

KLRE-1 genomic clone was isolated from a mouse genomic library using the KLRE-1 cDNA as a probe (cDNA sequence, first described by Koike et al[13]). The genomic DNA fragment from *Nsi*I site located at 1.5 kb upstream of the exon 2 (which contains ATG for first methionine) to *Bgl*II site present at 5.0 kb downstream of the exon 2 was used to construct the

From the Department of Molecular Immunology, the Department of Molecular Embryology, and the Department of Medical Immunology, Graduate School of Medicine, Chiba University, Chiba, Japan; RIKEN Research Center for Allergy and Immunology, Laboratory for Immune Regulation, Laboratory for Developmental Genetics, Tsurumi, Yokohama, Japan; and the Department of Immunology, Toho University, School of Medicine, Tokyo, Japan.

Submitted October 10, 2003; accepted March 22, 2004. Prepublished online as *Blood* First Edition Paper, April 6, 2004; DOI 10.1182/blood-2003-10-3468.

Supported by grants from the Ministry of Education, Culture, Sports, Science, and Technology (Japan): Grants-in-Aid for Scientific Research, Scientific Research A#13307011 (M.T.), B#14370107(T.N.), and Special Coordination Funds for Promoting Science and Technology (T.N.); the Program for Promotion of Fundamental Studies in Health Sciences of the Organization for Pharmaceutical Safety and Research, the Ministry of Health, Labor, and Welfare (Japan) (M.T.); and the Human Frontier Science Program Research Grant (RG00168/2000-M206) (M.T.).

E.S. and J.K. contributed equally to this study.

Reprints: Masaru Taniguchi, Laboratory for Immune Regulation, RIKEN Research Center for Allergy and Immunology, 1-7-22 Suehiro-cho Tsurumi-ku Yokohama-shi, 230-0045 Japan; e-mail: taniguti@rcai.riken.jp.

The publication costs of this article were defrayed in part by page charge payment. Therefore, and solely to indicate this fact, this article is hereby marked "advertisement" in accordance with 18 U.S.C. section 1734.

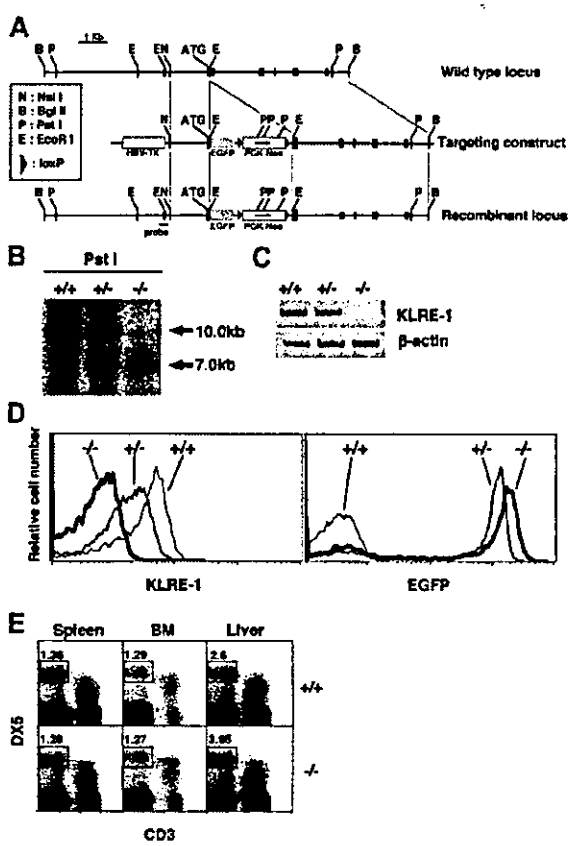

Figure 1. Characterization of KLRE-1 KO mice. (A) Generation of the EGFP–KLRE-1 knock-in mice. Schematic representation of the portion of the KLRE-1 gene locus (top), targeting construct (middle), and recombinant allele (bottom) including the relevant restriction sites. Probe used for Southern blot analysis is depicted. Exons are represented as black boxes. (B-E) Characterization of the EGFP–KLRE-1 knock-in mice. (B) Southern blot analysis. Southern blot analysis of *Pst* I-digested DNA from wild-type (WT) (+/+), heterozygous (+/−), or homozygous (−/−) KLRE-1 mice. DNA was hybridized with the probe shown in panel A to discriminate between the WT allele (10.0 kb) and the mutated allele (7.0 kb). (C) RT-PCR analysis for KLRE-1 mRNA. Total RNA prepared from DX5$^+$ splenocytes of WT (+/+), heterozygous (+/−), or homozygous (−/−) KLRE-1 mice was subjected to RT-PCR analysis on KLRE-1 and β-actin. PCR on β-actin assured an equal amount of cDNA. (D) Expression of KLRE-1 and GFP in the DX5$^+$TCRβ$^-$ splenocytes. The DX5$^+$TCRβ$^-$ splenocytes from WT (+/+), heterozygous (+/−), or homozygous (−/−) KLRE-1 mice were stained with the Cy5–anti–KLRE-1 (7E8) mAb. Expression of KLRE-1 (left panel) and EGFP (right panel) is shown as a histogram. (E) Normal development of NK cells in KLRE-1 knock-out (KO) mice. Spleen, bone marrow (BM), and liver mononuclear cells from WT (+/+) and homozygous (−/−) KLRE-1 mice were stained with the PE-DX5 and the Cy5–anti-CD3ε. The area representing NK (DX5$^+$ CD3ε$^-$) cells is shown with percentage.

targeting vector (Figure 1A). Enhanced green fluorescent protein (EGFP)–poly A cassette from the pEGFP-N3 vector (Clontech Laboratories, Palo Alto, CA) was amplified by polymerase chain reaction (PCR) and inserted in frame into the *Eco*RI site located at 39 bp downstream of ATG, followed by the neomycin-resistant gene (neo^r) cassette flanked by loxP sites. The targeting vector was electroporated into R1 embryonic stem (ES) cells, and G418-resistant clones were screened by Southern blotting with the 5′ external as well as the neo^r internal probes. Positive clones were aggregated with BDF1 blastocysts, and chimeric mice were obtained as described.[14]

Southern blot and PCR analyses

Genotyping was performed by Southern blotting or PCR using genomic DNA from the tail.[14] The probe for Southern blotting was synthesized by PCR with the primer set J03-23 (5′-AAGAGGGAATTCCAGGCACA-GATG-3′) and J03-35 (5′-GGGTGCTAAACGGAAATGTAAAGC-3′). The primers used for genotyping were GFP-6 (5′-CCTCTACAAATGTGG-TATGGC-3′) and GFP-8 (5′-ATGGTGAGCAAGGGCGAGGAGC-3′) for the targeted allele, and J03KO1 (5′-GATGGATGAAGCACCTGTAAC-3′) and J03KO3 (5′-TCAGAAACCCATCAGACCAACC-3′) for the wild-type allele. The primers for reverse transcriptase (RT)–PCR for KLRE-1 were J03-4 (5′-TAAGAGACAAGCAGGCACGCTGACTG-3′) and J03-7 (5′-ATGGATGAAGCACCTGTAACCCG-3′).

Cell preparation and flow cytometry

Splenic NK, spleen, bone marrow, and liver mononuclear cells were separated and stained with the appropriate antibodies as described[13,15]; phycoerythrin (PE)–anti-DX5, cyanin 5 (Cy5)–anti–T-cell receptor β (TCRβ), Cy5–anti-CD3ε (PharMingen, San Jose, CA), and Cy-5–labeled antibody against KLRE-1 (anti-NKG2I: 7E8) were used.[13]

Cytotoxic assay against the Con A blasts and BM cell engraftment

Cytotoxic assay against the Con A blasts and BM cell transfer experiments were performed essentially as described except that KLRE-1–deficient cells/mice were used in some experiments.[13]

Results and discussion

Establishment of EGFP–KLRE-1 knock-in mice

We have generated enhanced green fluorescent protein (EGFP)–KLRE-1 knock-in mice to rigorously assess the function of KLRE-1. Southern blot analysis with the 5′ external probe confirmed the correct recombination (Figure 1B). RT-PCR and flow cytometry analyses demonstrated that there was no detectable KLRE-1 transcript or surface expression in the homozygous mice (Figure 1C-D, −/−). A slight decrement of the expression was observed in the heterozygous mice (Figure 1D, left panel, +/−). Concomitantly, the expression of GFP was inversely correlated with the loss of KLRE-1 expression (Figure 1D, right panel). Mice homozygous for EGFP–KLRE-1 (KLRE-1–deficient mice) were born at the expected frequency and were fertile, with no apparent growth abnormality (data not shown). Regarding NK cells, no difference in the profile of CD3/DX5 expression in the spleen, bone marrow (BM), and liver mononuclear cells was noticed between wild-type littermates and knock-out mice (Figure 1E). In addition, no significant variation in the number or ratio of lymphoid subsets was detected in thymus, spleen, and BM cells, suggesting that KLRE-1 is dispensable for the development of lymphoid cells (data not shown).

KLRE-1 is critical for NK cell–mediated allorejection

Previous reports indicate that KLRE-1 plays a pivotal role in allogeneic or redirected lysis.[12,13] Therefore, the roles of KLRE-1 in cytotoxic activity against allogeneic lymphocytes were assessed using KLRE-1–deficient cells. Lymphokine activated killer (LAK) cells from C57BL/6 wild-type mice were mixed with BALB/c Con A blasts, and cytotoxic activity was examined. While wild-type LAK cells showed a significant cytolytic activity against allogeneic target cells, LAK cells from KLRE-1–deficient mice showed little activity (Figure 2A, left panel). In the syngeneic system, however, no marked difference in the cytotoxicity between wild-type and KLRE-1–deficient cells was observed (Figure 2A, right panel). These results demonstrate that KLRE-1 is crucial for NK cells to exert allogeneic cytolytic activity.

We have further explored the function of KLRE-1 in allogeneic BM cell transplantation using KLRE-1–deficient mice (Figure 2B-C). BALB/c BM cells infused to the lethally irradiated C57BL/6

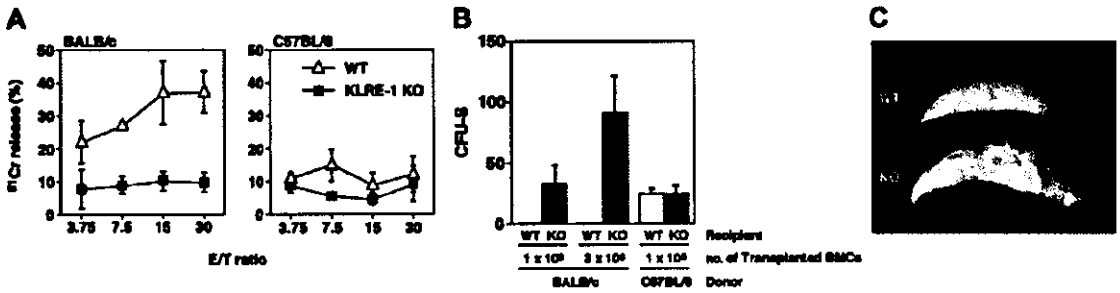

Figure 2. KLRE-1 plays a pivotal role in allogeneic bone marrow transfer. (A) Cytotoxic activity against allogeneic Con A blasts using KLRE-1–deficient cells. Cytolytic activity of LAK cells containing activated NK cells from wild-type C57BL/6 (WT, △) and KLRE-1–deficient (KLRE-1 KO, ■) mice was assessed. Representative data from 3 independent experiments (n = 5/experiments) are shown as means ± SD. (B-C) KLRE-1 KO mice fail to reject BM allograft. (B) BALB/c BM cells (1×10^6 or 3×10^6 cells) or C57BL/6 BM cells (1×10^5 cells) were intravenously infused to lethally irradiated age-matched wild-type or KLRE-1–deficient C57BL/6 mice. At 8 days after transplantation, spleens were removed and the number of colonies on the spleen was counted. Representative data from the 3 independent experiments are shown. Data are indicated as means ± SD of 5 individuals per experiments. (C) Representative picture of allograft-induced colony formation in the spleen of KLRE-1 knock-out mice. Colony formation resulting from the BALB/c BM allograft as described in panel B can be observed on the spleen of lethally irradiated KLRE-1 null mice (KO), but not on that of C57BL/6 mice (WT) after the fixation in the Bouin solution. The photo was taken with a Nikon digital camera (Cool Pix 995) and processed with Adobe Photoshop.

mice were rejected, and no colony formation was seen in the spleen of C57BL/6 mice (Figure 2B-C, WT). In sharp contrast, when BALB/c BM cells were transferred into KLRE-1–deficient mice, a graft dose-dependent colony formation was observed, indicating that the rejection of grafts was severely compromised due to the absence of KLRE-1 (Figure 2B-C, KO). When syngeneic cells were used, the graft was accepted irrespective of KLRE-1 absence and resulted in the formation of a similar number of colonies (Figure 2B, rightmost column). Taken together, one can conclude that KLRE-1 is a crucial mediator for the allograft rejection in vivo.

KLRE-1 has been reported as an inhibitory NK receptor due to its association with the protein tyrosine phosphatase, Src homology domain containing tyrosine phosphatase 1 (SHP-1), and cross-linking of KLRE-1 inhibits NK cell–mediated cytotoxicity.[12] In our hands, however, KLRE-1 functions as an activating receptor. In fact, cross-linking of NKG2I together with the addition of interleukin-2 (IL-2) and/or IL-12 culminates in the production of interferon γ (IFN-γ).[13] The inhibition of the cytotoxicity observed in redirected lysis assay may most likely mirror the fact that the absence of KLRE-1 perturbed NK cell–mediated cytotoxicity against allogeneic cells[12] (Figure 2A, left column). As KLRE-1 is devoid of any signaling motif such as immunoreceptor tyrosine-based inhibitory motif (ITIM) or immunoreceptor tyrosine-based activation motif (ITAM), further works should be necessary to decipher whether KLRE-1 functions as an inhibitory receptor or activating receptor.

In summary, we have shown that KLRE-1 is critical for NK cells to exert allogeneic recognition and rejection using KLRE-1–deficient mice.

References

1. Murphy WJ, Kumar V, Bennett M. Rejection of bone marrow allografts by mice with severe combined immune deficiency (SCID): evidence that natural killer cells can mediate the specificity of marrow graft rejection. J Exp Med. 1987;165: 1212-1217.
2. Trinchieri G. Biology of natural killer cells. Adv Immunol. 1989;47:187-376.
3. Lanier LL. NK cell receptors. Annu Rev Immunol. 1998;16:359-393.
4. Yokoyama WM. Natural killer cell receptors. Curr Opin Immunol. 1998;10:298-305.
5. Toyama-Sorimachi N, Taguchi Y, Yagita H, et al. Mouse CD94 participates in Qa-1-mediated self recognition by NK cells and delivers inhibitory signals independent of Ly-49. J Immunol. 2001; 166:3771-3779.
6. Raziuddin A, Longo DL, Mason L, Ortaldo JR, Bennett M, Murphy WJ. Differential effects of the rejection of bone marrow allografts by the depletion of activating versus inhibiting Ly-49 natural killer cell subsets. J Immunol. 1998;160:87-94.
7. Makrigiannis AP, Gosselin P, Mason LH, et al. Cloning and characterization of a novel activating Ly49 closely related to Ly49A. J Immunol. 1999; 163:4931-4938.
8. Makrigiannis AP, Etzler J, Winkler-Pickett R, Mason A, Ortaldo JR, Anderson SK. Identification of the Ly49L protein: evidence for activating counterparts to inhibitory Ly49 proteins. J Leukoc Biol. 2000;68:765-771.
9. Daniels KA, Devora G, Lai WC, O'Donnell CL, Bennett M, Welsh RM. Murine cytomegalovirus is regulated by a discrete subset of natural killer cells reactive with monoclonal antibody to Ly49H. J Exp Med. 2001;194:29-44.
10. Van Beneden K, Stevenaert F, De Creus A, et al. Expression of Ly49E and CD94/NKG2 on fetal and adult NK cells. J Immunol. 2001;166:4302-4311.
11. Wilhelm BT, Mager DL. Identification of a new murine lectin-like gene in close proximity to CD94. Immunogenetics. 2003;55:53-56.
12. Westgaard IH, Dissen E, Torgersen KM, et al. The lectin-like receptor KLRE1 inhibits natural killer cell cytotoxicity. J Exp Med. 2003;197:1551-1561.
13. Koike J, Wakao H, Ishizuka Y, et al. Bone marrow allograft rejection mediated by a novel murine NK receptor, NKG2I. J Exp Med. 2004;199:137-144.
14. Akasaka T, Kanno M, Balling R, Mieza MA, Taniguchi M, Koseki H. A role for mel-18, a Polycomb group-related vertebrate gene, during theanteroposterior specification of the axial skeleton. Development. 1996;122:1513-1522.
15. Kaneko Y, Harada M, Kawano T, et al. Augmentation of Valpha14 NKT cell-mediated cytotoxicity by interleukin 4 in an autocrine mechanism resulting in the development of concanavalin A-induced hepatitis. J Exp Med. 2000;191:105-114.